Platinum-palladium catalysts for methane-fuelled heaters

by

Xiaoxing Wu

A thesis submitted in partial fulfillment of the requirements for the degree of

Master of Science

in

Chemical Engineering

Department of Chemical and Materials Engineering

University of Alberta

Abstract

Natural-gas fuelled catalytic heaters are commonly used in heating industrial space and remote location operations. Industrial units typically contain platinum that provides methane combustion at lower temperatures than non-catalytic burning. This work aimed to find a cost-efficient alternative to monometallic platinum catalyst by replacing some of platinum with less expensive palladium, which is also known for methane combustion activity. The task is complicated by non-uniform reactant profiles across the catalytic pad. Several Pd:Pt bimetallic catalysts were prepared by dry impregnation of commercial pads with metal precursors and tested in methane combustion with 5% water presence at two different methane-to-oxygen molar ratios (0.2 and 0.02). $Pt_{1.6}Pd$ catalyst (molar ratio) is recommended to replace monometallic platinum: it provides higher activity than monometallic Pt catalyst at 0.02 CH_4-to-O_2 ratio. At the 0.2 ratio, its activity is lower than that of Pt, but is sufficient for adequate heater operation.

Acknowledgement

The support and guidance from my supervisors, Dr. Natalia Semagina and Dr. Robert Hayes, are highly appreciated. They have been helpful all through my Master program. I would also like to thank Dr. Jing Shen for her advices and guidance when I started my project and helped me with the TEM test.

Financial support of this project from NSERC strategic grant is gratefully acknowledged.

Table of Contents

List of Tables

List of Figures

Nomenclature

T	Temperature
$\triangle H$	Enthalpy
atm	Atmospheric pressure
K	Kelvin
No_x	Nitric oxide and nitrogen dioxide
vol. %	Volume percentage
wt. %	Weight percentage

Abbreviations

DFT	Density functional theory
FID	Flame ionized detector
FL	Fuel lean
FR	Fuel rich
GC	Gas chromatograph
HC	Hydrocarbon
HTA	Hydrothermal aging
TCD	Thermal conductivity detector
TEM	Transmission electron microscopy
TOF	Turn over frequency
TPR	Temperature programmed reduction
WHSV	Weight hour space velocity
XPS	X-ray photoelectron spectroscopy
XRD	X-ray diffraction

1. Introduction

In the past years, natural gas has attracted considerable attention in the energy sector. Natural gas is a hydrocarbon gas mixture consisting primarily of methane (CH_4), which is a clean and highly efficient energy for transportation, heating and so on. Methane combustion in heating applications has some disadvantages: fire risk, poisonous gas producing and high energy loss. To overcome the disadvantages, catalytic burners have been developed that use solid catalysts to burn methane without an open flame. The catalytic heaters, in turn, pose a risk of incomplete combustion (due to the lower temperature compared to the traditional thermal burner) and require expensive catalysts.

Platinum group metals are known to be the most active catalysts used for the methane combustion. Monometallic platinum catalysts may provide 100% methane conversion at temperatures as low as 400 °C, depending on many affecting factors. Palladium, which is normally more active than platinum, is also an efficient catalyst for methane combustion with less than half of platinum price. Replacement of some Pt with Pd is a way to reduce the cost of catalyst used in catalytic burner. However, the platinum replacement may lower the fuel conversion.

This work aims to replace some of the platinum with palladium for applications in catalytic heaters and uses methane combustion at two different methane-to-oxygen ratios to imitate different regimes of the unsteady heater operation. The objective is to find a balance between the catalyst cost by introducing lower-cost palladium to platinum and catalyst activity, so that the bimetallic catalyst is active enough to get 100% conversion in different regions of a catalyst pad. How the mono Pt, Pd and bimetallic Pt-Pd catalysts with different ratios of Pt versus Pd would behave under different conditions, with and without inhibiting water presence, and catalyst stability were studied in this research.

2. Literature review

2.1 Natural gas

Nowadays, the natural gas has become more and more popular in energy area. The use of methane (CH_4), which is the main component of natural gas, with four C-H bonds and one carbon atom, leads to the lowest carbon dioxide emission producing the same amount of energy for methane combustion [1]. Methane combustion has been used in house heating, transportation facilities and so on. However, natural gas combustion has some disadvantages. While burning natural gas, the carbon might not be burnt completely and CO will be produced; nitrogen will turn into NO_x after combustion at high reaction temperature [2]. Also, the incomplete combustion of methane might happen and some methane goes into the atmosphere and cause a serious problem, since the methane is 23 times more efficient in greenhouse effect potential compared with carbon dioxide [3]. The challenges may be overcome by using a catalytic burner, which reduces CO, HC, NO_x emission and enhance methane conversion.

2.2 Catalytic burner

2.2.1 Advantages and disadvantages

For hydrocarbon combustion such as methane, propane and others, the open flame combustor was originally used. As attention towards the environmental impact of many technologies began to grow, several disadvantages were identified with these homogeneous combustion units according to J. D. MacConnell [4]. It has a large fire risk since it uses an open flame in the burner which restricts where it may be used to areas with few flammable materials [4]. More importantly, the temperature of the flame may, in some circumstances, exceed a temperature of 1000 °C. This leads to a considerable energy loss of heat to the surrounding environment, as well as the more minor losses associated with the emission of visible light

energy. Also, the high temperature combustion is likely to rise the NO_x emissions by a considerable amount, which is against the increasing emission standards of fuel burner.

To solve the problems mentioned above, a catalytic burner was developed. The catalysts in the heater enable fuel oxidation to take place at a substantially lower temperature. For example, the combustion of propane can take place with the presence of catalysts at about 650 K, which would be about 1250 K without the aid of catalysts [4].

Low temperature fuel combustion has several advantages. Firstly, catalytic combustion has no flammability limits. This will extend the usage of the catalytic burner to areas where using a flame-based burner would be unwise. Also, at low temperature, the NO_x emission is abated. Maximum carbon monoxide levels emitted are also nearly negligible at only a few parts per million [5]. At a time when environmental awareness is quite important, the catalytic combustor is a quite attractive alternative to the flame combustor as it can be operated to be nearly pollutant free.

The catalytic heater is able to compensate for the disadvantages of the traditional open flame combustor. However, the catalytic combustor, in the present state of development, has some disadvantages. It can result in raw fuel emission into the atmosphere if there is incomplete combustion. The emissions are an environmental hazard and is also an indication of combustion inefficiency. To some extent, these emissions can be controlled by altering the ratio of fuel and air in the reactant mixtures, however this may unfortunately result in higher combustion temperatures and increased carbon monoxide by-product.

2.2.2 Combustor system

There are typically two stages in a conventional combustion system. The objective of the first stage is to generate useful energy in the form of heat and/or power. This is referred to as primary combustion. It is followed by secondary combustion, whose purpose is to clean the emissions prior to release to atmosphere.

For catalytic combustors, there are two means to provide the necessary reactants. One is to

pre-mix the combustible gas with sufficient oxygen and supply this combined feed to the reactor [6]. Other methods can be used to varying degrees of efficiency to provide the proper amount of oxygen for combustion, such as supplying fuel at the inlet and providing the necessary oxygen through a counter-diffusive reactor system [7]. Fig. 2.1 shows the design of one gas supply way.

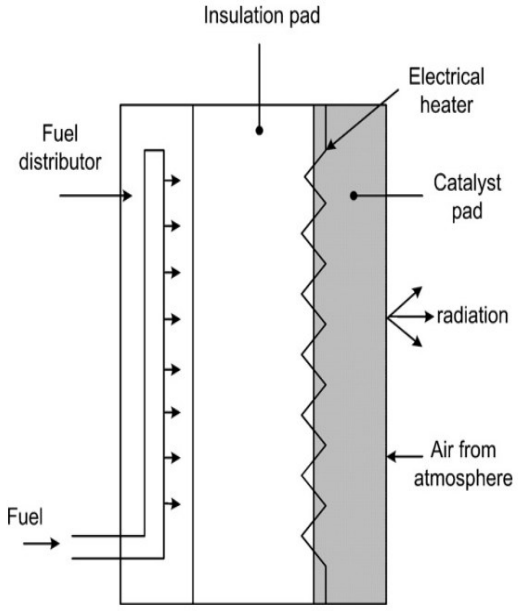

Fig. 2.1. Schematic of a counter-diffusive reactor. Reprinted with permission from [7].

2.2.2.1 Catalytic radiant reactor

Typical feedstocks for catalytic radiant burners are usually methanol, natural gas, propane, et al. From Fig. 2.1 it is shown that the fuel and air are mixed together before going into the reactor. Presently noble metal catalysts are often used for combustion. These catalysts are coated onto a fibrous structure that serves as the reaction zone. The heat produced by the reaction zone is expelled into the surrounding environment via a heat removal system.

The central component of the entire unit is the fibrous support structure. Its purpose is to separate the reactor zone from the incoming reactant gas mixture, and remove the possibility of combustion of the reactant gas before the catalyst bed. An added advantage of using the fibrous support structure is that it ensures the homogeneous distribution of fuel and combustion air. The

reaction conditions are established uniformly due to unform distribution, which leads to the abatement of pollutant emissions. Moreover, the shape of the heater is predefined by a stable fibrous structure using highly porous ceramic parts.

Pt is a noble metals that remain in their metallic forms under oxidation conditions. As an example of commercial heaters, several catalysts of platinum group were developed by Matthey Bishop Inc. [4] , which are called Cataheat. The catalysts applied in the reaction zone are usually impregnated by these two noble metals. The catalyst is impregnated onto the fibrous structure in the form of a wash-coat powder. The wash-coat powder, which typically consists of γ-Al_2O_3, has two primary advantages: it enlarges the catalyst surface allowing for a greater surface-to-volume ratio and it reduces the possibility of sintering of nanoparticles which would lead to catalyst deactivation. These advantages allow for a very small particle distribution and thermal stability.

In the research done by Marc D. Rumminger, et al [8], a multiple-layer porous medium is placed in a radiant burner. An oxidizing catalyst is put on one layer of them. They found the efficiency is raised significantly when put the catalyst layer on the downstream edge of the porous medium. Also, the catalyst layer need to be placed in a high temperature zone. Negligible improvement of efficiency for radiant is gained otherwise.

2.2.2.2 Counter-diffusive reactor

As shown above, diffusion burners have air flow externally across the combustion reactor and the oxygen flows to the porous structure through the boundary layer. Often an electrical heater is required to preheat the catalyst bed in order to properly initialize reaction. Under suitable concentration, catalyst and temperature conditions, the fuel combustion will take place near the surface. Radiation serves as primary means of transferring heat to the surrounding environment [6]. Typically diffusion burners are used during recreational activities where their mobility and lack of open flame make them a safe choice.

N. Jodeiri et al [7] developed a two-dimensional model for a counter-diffusive reactor to study diffusions of oxygen and methane. The catalyst is loaded on a fiber pad packed at the back

of reactor. Fuel is fed from the inlet of the reactor. Oxygen comes from the exit of the reactor. When fuel and oxygen meet with each other in the catalyst pad area, combustion happens and the heat is produced. As seen from Fig. 2.2 and 2.3, the middle part of the pad has higher temperature and the bottom area have the highest. Also, with the increase of flow rate, the maximum temperature drops. The higher fuel flow rate, the closer the position of maximum temperature is to the outlet of the reactor.

The mass fraction of oxygen falls rapidly with distance from the front (Fig. 2.4), which indicates that the reaction happens mainly in the front part. This is consistent with the temperature profile, for more reaction leading to higher temperature. Also, the increase of the fuel flow rate leads to the faster consumption of oxygen. Contrast to oxygen mass fraction profile, mass fraction profile of methane shows a different trend. The change of methane is a gradual drop from the back of the reactor.

The water concentration distribution has a maximum near the area of maximum temperature. Increase the fuel flow rate would cause a lower water concentration at the back of the reactor and a higher maximum water concentration in the front part of reactor. And carbon monoxide concentration is similar to water concentration distribution profile.

According to their research, the methane conversion varies with fuel flow rate. Higher fuel flow rate decrease the methane conversion. It might be explained by the shorter reaction time between fuel and air at higher fuel flow rate.

Fig. 2.2 is a temperature profile across the pad. The two dash lines are the interfaces between the porous medium and insulation blanket, the right one at the position of 0.056 m marks the boundary of insulation pad and catalyst pad. Q is the methane feed flow rate, Y refers to the height from the reactor bottom. It is seen that at 0.024 m above the bottom of reactor, the temperature got the highest number in the catalyst pad area. The temperature decreased rapidly when it gets closer to the back of reactor. This result is reasonable since near the front of reactor, oxygen and fuel have a ratio that is suitable for combustion.

Fig. 2.3 shows that the maximum temperature moves towards the back of the pad when

methane flow rate decreases. Also with lower flow speed, the combustion efficiency increased proved by the higher maximum temperature of the slower flow rate.

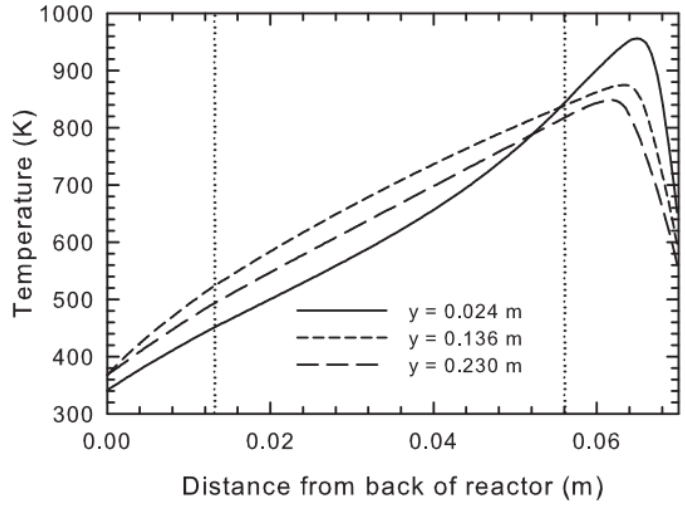

Fig. 2.2. Temperature profiles along the reactor at the reactor bottom at three flow rates of methane. Reprinted with permission from [7].

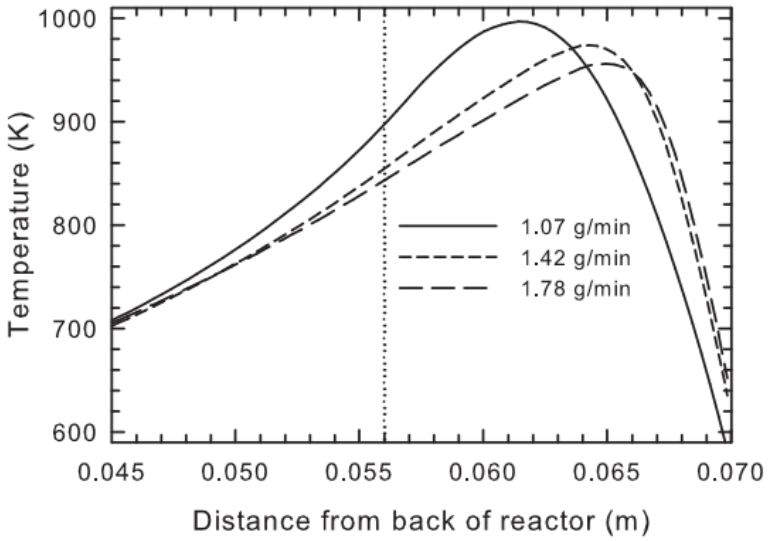

Fig. 2.3. Temperature profiles along the reactor at 0.136 m from the reactor bottom at three flow rates of methane. Reprinted with permission from [7].

Fig. 2.4 shows the methane/oxygen ratio along the reactor. The figure was developed based on data from [7]. As seen, there are fuel-rich and fuel-lean regions across the pad. Overall,

diffusion is important in the operation of the reactor. The primary limiting step of the methane conversion is the mass transfer of oxygen through the external boundary layer in the front of the reactor. With more oxygen present in the reaction area, the fuel is able to combust more completely.

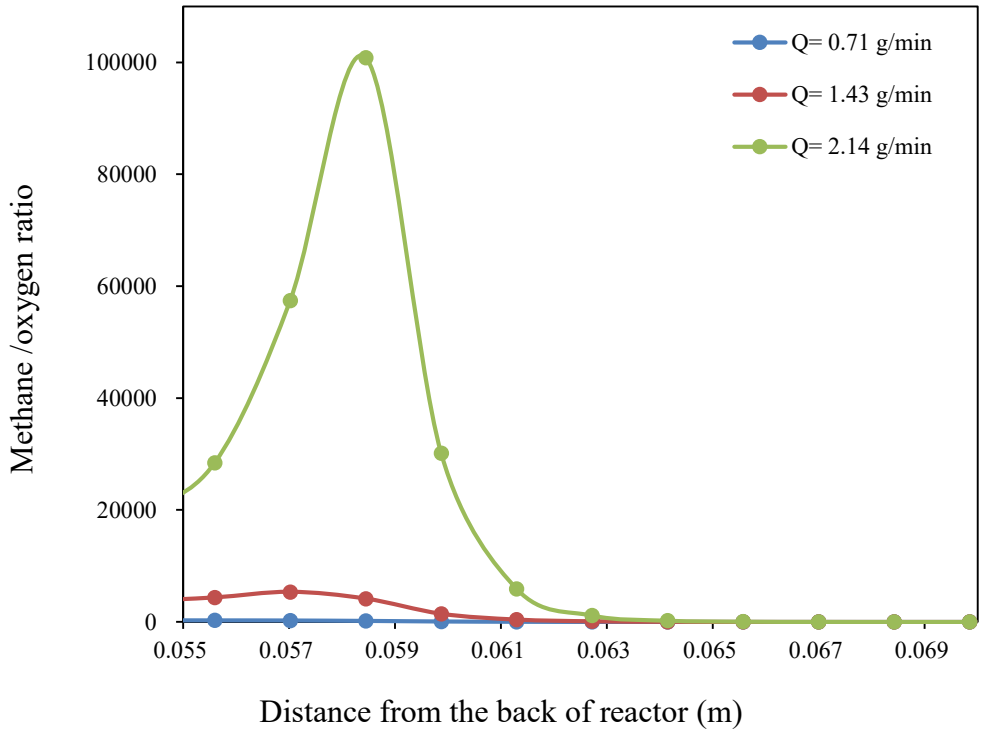

Fig. 2.4. Methane/oxygen molar ratio along the reactor at a height of 0.15 m from the reactor bottom, based on data from [7].

2.3 Mechanism of catalytic methane combustion

2.3.1 Main reaction

Ideal reaction for lean combustion of methane is:

$$CH_4+2O_2 \rightarrow CO_2+2H_2O \quad \Delta H^{o}_{298}= -192 \text{ kcal/mol} \quad (1)\ [1]$$

The bond strength of the C-H bond in the methane molecule is 104 kcal mol^{-1}. This is a quite high activation energy for a thermal reaction. On the other hand, apparent activation energy for

the dissociative adsorption of methane on certain crystalline material is only 7-10 kcal/mol [1]. With the help of catalyst, the methane will dissociate on the surface on the catalyst and then react with oxygen, which is much easier considering the activation energy.

However, in reality, due to the water vapor in air and water generation during the reaction, the reaction speed and conversion are inhibited [9].

2.3.2 Pd and PdO

Among the Pt group metals used for the catalytic methane combustion, the majority of literature on the reaction mechanism concerns Pd catalysts. The apparent activation energy for methane combustion over crystalline PdO is 17-20 kcal/mol (initially dry), while over metallic Pd, it is 40-45 kcal/mol [1]. It shows that the reaction rate is higher with dry crystalline PdO.

On the PdO surface, the reaction has been observed to involve lattice oxygen, suggesting a redox mechanism. Also, methane might be adsorbed on oxygen vacancy states on the PdO surface [10].

Metallic palladium and crystalline oxidized phases of palladium have very different crystal structures, which has a strong influence on the oxidation and reduction process. Metallic palladium has an fcc lattice structure, with the lattice parameter a=0.38898 nm at 298 K [11]. The distance between the neighboring palladium atoms is 0.275 nm. In comparison, the relative distance of hydrogen and carbon atoms in methane molecule is 0.189 nm. The lattice parameters for crystalline PdO at 298 K are a=b=0.3043 nm and c=0.5337 nm. In the PdO crystal, the shortest distance between the Pd atoms in the PdO (101) surface is 0.343 nm. The density of the Pd atoms in the metallic structure is nearly twice as high as that for PdO crystal. Therefore, oxidation of the bulk of the metallic crystallite needs a major restructuring of the crystal lattice with a significant increase in the unit volume and major expansion of the palladium lattice.

According to Bayer et al [12], the PdO phase is stable under 1050 K in 1 atm with the O_2 partial pressure of 0.21 atm , and the metallic Pd is stable at higher temperatures. In the work of Peuckert [13], PdO decomposition and crystalline PdO formation was studied using X-ray

photoelectron spectroscopy (XPS). The PdO decomposition happened at about 425 K and 750-775 K. There is an intermediate state, having a Pd/O ratio near 0.7 for the formation sample and 0.4 for the decomposition sample.

The interfacial tension between metallic Pd and alumina is less than that for PdO and alumina. At low coverages, the PdO phase is known to spread over the support, while the metallic Pd phase forms larger, more segregated crystallites [14]–[16].

Several different Pd/oxide structures have been discovered under different conditions [17]–[21]. The adsorption energy of oxygen on the surface has been estimated about 55 kcal/mol [22]. In air at 1 atm, the formation of bulk PdO occurs only at about 625 K. For the crystalline PdO, it's stable below 1046 K in air at 1 atm. PdO formation over a large range of temperatures experienced in practical application is rate controlled.

Legare et al. [23] used X-ray photoelectron spectroscopy, ultraviolet photoelectron spectroscopy, and Auger electron spectroscopy techniques to study the interaction of oxygen and palladium. At 298 K and 10^{-6} Torr oxygen pressure, oxygen was only adsorbed on the catalyst surface. At about 575 K and 10^{-2} oxygen pressure, the oxygen penetrated into the Pd subsurface. The crystalline PdO was only observed at 625 K with 1 atm oxygen pressure.

According to Dragos Ciuparu et al [1], the oxidation of Pd (111) proceeds through a three-step mechanism:

(1) Rapid adsorption that stops at 0.25 monolayer (ML, 1 ML=1 O atom/surface Pd atom) of atomic oxygen;

(2) Oxygen penetration into the surface is accompanied by island growth leading to the formation of two phases that are intermediate between Pd and PdO;

(3) Formation of bulk PdO.

There is only one type of oxygen species for (001) and (110) bulk-terminated surfaces: oxygen atoms bridge bound to two Pd atoms.

2.3.3 Methane oxidation pathways and water inhibition

Fig. 2.5 shows how methane oxidation rates change with the concentrations of CH_4, O_2, CO_2 and H_2O. Methane activity has nearly proportional relationship with CH_4 concentration (1.1 ± 0.1 order), while methane oxidation depends weakly on O_2 concentration (0.1 ± 0.1 order) [24]–[26]. CO_2 has negligible effect on the reaction rate. Water inhibits reaction significantly according to the figure.

Ribeiro et al developed a rate law for methane combustion on Pd [25]. This law (equation (1) is consistent with Fig. 2.5.):

$$r = k\,(CH_4)^{1.0}(O_2)^{0}(H_2O)^{-1.0} \qquad (2)$$

Fig. 2.6 and Fig. 2.7 illustrate the surface reaction mechanism, including water inhibition [27]. Fig.2.6 shows the dissociative chemisorption on a site pair consisting of adjacent Pd surface vacancies and surface Pd-O species.

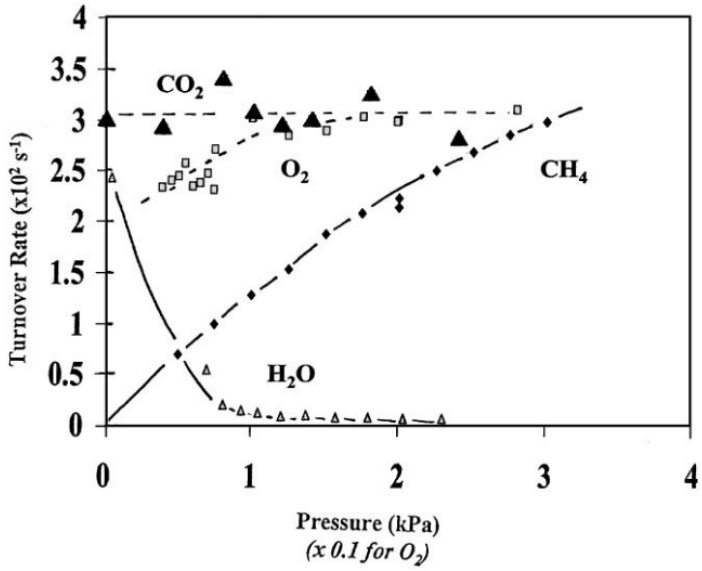

Fig. 2.5. Effects of CH_4, O_2, H_2O, and CO_2 on methane oxidation rates. Reprinted with permission from [27].

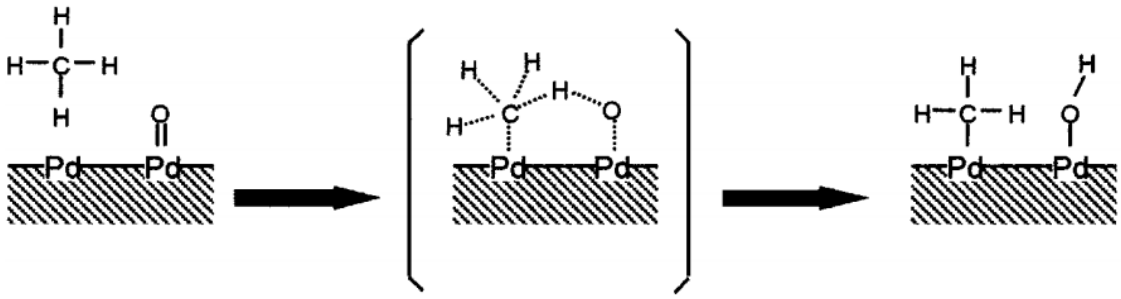

Fig. 2.6. Methane dissociation on a surface Pd–PdO site pair. Reprinted with permission from [14].

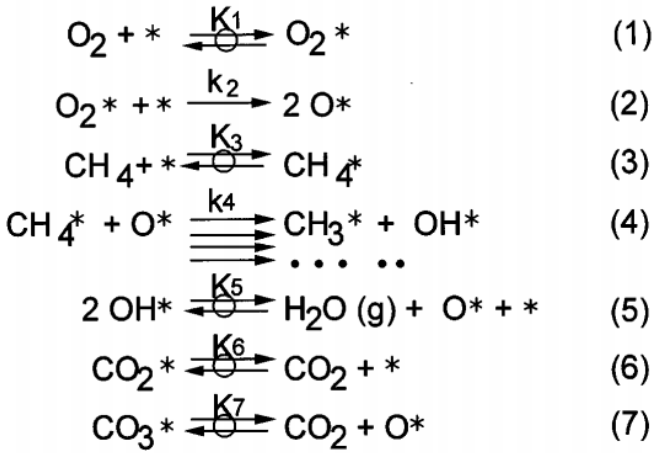

Fig. 2.7. Methane oxidation reaction pathways. Reprinted with permission from [14]. (Asterisks stand for oxygen vacancies on PdO surfaces)

Fig. 2.6 is the detailed scheme of the steps 3 and 4 in Fig. 2.7. This dissociative chemisorption of methane (step 4) is the rate determining step for methane oxidation. Physisorbed methane molecule interacts with coordinatively unsaturated Pd sites (*) and then the Pd-O surface species abstract one of the H atom from methane molecule to form surface hydroxyl groups (Pd-OH).

The step 4 in Fig. 2.7, which is rate determining step, is determined by the concentrations of CH_4*, O* and OH*. With more CH_4* and O* species, the rate increases, explaining the positive effects of methane and oxygen concentration on methane oxidation rate. On the other hand, the

increase of OH* leads to the decrease of the reaction rate. To reduce the hydroxyl group concentration, water is formed by quasi-equilibrated condensation of OH* (step 5) and regenerate surface vacancies. With water presence, the reaction of step 5 is inhibited, leading to the high concentration of OH* and absence of surface vacancies, and finally overall inhibit the methane oxidation process.

Thus, water inhibits turnover rate by titrating vacancies which activate the rate determining step of methane oxidation. The density of such vacancies is controlled by the quasi-equilibrated desorption of H_2O and with the increasing concentration of water, the number of available sites decreases.

2.4 Platinum catalysts versus palladium catalysts

Platinum and palladium display different activity in methane combustion. Methane combustion on Pt is first order to methane zero order in oxygen pressure; oxygen adsorption on Pt is fast and irreversible below 400 °C, while methane adsorption is slow.

For completely dispersed Pt catalyst, it starts oxidizing at 300 °C and converts into PtO_2. For crystallite Pt catalyst, only surface is oxidized when heated up to 600 °C and the catalyst is usually covered with adsorbed oxygen. So methane oxidation activity of dispersed Pt catalyst is 10-100 times lower than crystallite Pt catalyst (Table 2.1).

Table 2.1. Comparison for two kinds of Pt catalysts in methane combustion

Catalyst	Turn over frequency, s^{-1}	Apparent activation energy, kcal/mol
Dispersed Pt	0.005	36
Crystallite Pt	0.08	28

The formation of the two phases depends on the support composition, the metal salt used, the amount of metal deposited, and the conditions of oxidation and reduction of the catalyst.

2.4.1 Structure sensitivity on methane combustion on platinum

Methane oxidation over platinum is a structure-sensitive reaction according to Hicks et al [28]. With different structures, the turnover frequency of the platinum catalysts varies by two orders of magnitude.

Under methane combustion reaction conditions, the platinum surfaces are covered with oxygen. On the other hand, methane adsorption process is much slower. Therefore when the oxygen/methane ratio is above 2, methane is completely replaced by oxygen. It suggests that the structure sensitivity of methane oxidation should be related to differences in the reactivity of the adsorbed oxygen.

Two phases of platinum coexist on the catalysts supports: a dispersed phase, and a crystalline phase. The dispersed phase is stabilized by alumina, and is responsible for the 2068 cm^{-1} peak of carbon monoxide adsorption infrared spectrum. The crystalline phase doesn't have much interaction with the support, and is responsible for the 2080 cm^{-1} peak of carbon monoxide adsorption infrared spectrum [29]. According to Hicks et al [28], the turnover frequencies have strong correlation with the infrared spectrum of adsorbed carbon monoxide. A broad peak at 2068 cm^{-1} corresponds to low turnover frequencies, and the 2080 cm^{-1} peak is corresponds to high turnover frequencies. Therefore, the crystalline platinum phase have higher turnover frequencies compared to the dispersed phase. The crystalline platinum has 10 to 100 times higher methane oxidation activity of that of dispersed phase [28].

During reaction process, the dispersed phase platinum is oxidized to PtO_2 starting at 300 °C [30]–[32]. For the platinum crystallites, only the top two surface layers are oxidized when heating in air to 600 °C [24], [30], [31], and the whole crystallites are covered with adsorbed oxygen.

Their sizes have negligible impact on the oxidation process. A study about oxygen adsorption is conducted by Gland et al [33]. In the study, oxygen adsorption was tested separately on flat and stepped Pt (111). The energy of adsorption of flat platinum was the same with that of stepped Pt (111), which suggests that the reactivity of oxygen adsorption doesn't change with the atom location of the crystallites. In other words, the reactivity of the adsorbed oxygen should not change with crystallite size.

The relative amount of the dispersed phase and the crystalline platinum phase depends on the support composition and the preparation methods.

2.4.2 Structure sensitivity on methane combustion on palladium

Palladium catalyst activity varies with the structure by the factor of 280. The turnover frequencies depend on palladium particles size.

The Pd particle size can be characterized by the ratio of linear/bridged adsorption mode of carbon monoxide, as determined by infrared spectroscopy. When increasing the particle size, the linear/bridge peak ratio decreases. The linearly bonded carbon monoxide band is attributed to adsorption on all types of sites [34], while the bridged bonded band is attributed to adsorption on the faces of palladium crystals. In other words, the small crystallites with more corner and edge sites have higher linear to bridge peak ratio, and the ratio of linearly bonded to bridge bonded of the large crystallites with less corner and edge sites and more face atoms is lower.

Under oxidizing conditions, the palladium particles oxidizes partly between 200 °C and 900 °C. At 300 °C and 110 Torr of oxygen, small crystallites are converted into dispersed PdO completely, while large ones are only oxidized partially [28]. The partially oxidized palladium is broken into smaller crystallites covered with absorbed oxygen.

Roth et al [35] conducted experiments for total oxidation of methane on Pd/Al_2O_3. Fig. 2.8 shows the turnover frequency (activity per surface palladium atom measured from H_2 chemisorption on reduced particles) versus mean particle size of Pd/Al_2O_3. For the particles

smaller than 12 nm in diameter, the mean particle size and the turnover frequency have a linear relationship. It suggests that in this diameter range, the larger the particle is, the more active it is. When the mean particle size is larger than 15 nm, the turnover frequency drops from around 60/h to 40/h and remains constant with the increase of mean particle size.

This figure suggests that the large and small palladium particles have different catalytic properties. For large particles, the catalytic activity mostly depends on the geometric surface area of PdO/Pd particles size. The TOF is constant because the surface PdO film layer is considered to be highly reactive for methane. For small particles, the reason that TOF has a linear relationship with mean particle size is that the density and stability of oxygen vacancies of PdO_x surface determine the methane oxidation turnover rate based on the study of Fujimoto et al [27]. On the other hand, Pd-O bonds, which would increase with decreasing PdO_x particle size, would determine the density of vacancies. That may explain the linear relationship between TOF and particle size for small particles.

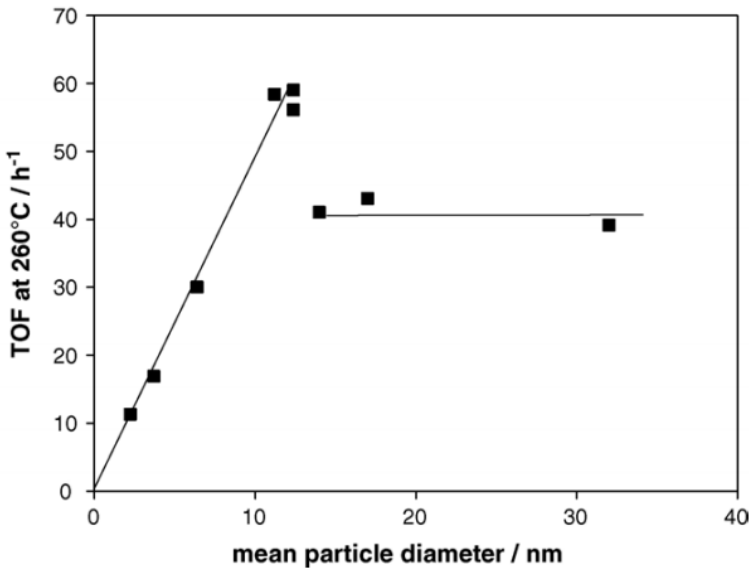

Fig. 2.8. TOF of Pd/Al_2O_3 catalysts versus mean particle diameter. Reprinted with permission from [35].

The size of the palladium crystallites depend on the support composition and method of

preparation.

However, there is a controversy in literature regarding the reaction structure sensitivity. For example, R. Burch et al [36] found that methane conversion is independent of particle sizes. The controversy may be explain by the use of chlorine or chlorine-free metal precursors, feed impurities, support effects and uncertainty of metal particle size that may change under high-temperature oxidative conditions.

2.5 Effect of fuel lean and fuel rich conditions on the combustion activity

R. Burch et al [36] used chlorine-free precursors to prepare Pt/Al_2O_3 and Pd/Al_2O_3 catalysts and tested these catalysts under fuel lean, stoichiometric and rich conditions.

The particle size of support Al_2O_3 were between 250 and 850 μm. After dry impregnation and drying in an oven at 120 °C for 2 h, the catalysts were calcined at 500 °C for 2 h (Pt catalysts) and 17.5 h (Pd catalysts). Three different O_2/CH_4 ratios were used: 5:1 (fuel lean), 2:1 and 1:1 (fuel rich) for the methane combustion. The metal nanoparticle sizes were in the order of 2 – 4 nm.

When testing under O_2/CH_4 ratio of 5:1 mixture (2000 ppm methane), the hysteresis between ignition and extinction curves on a 4% Pt catalyst was 25 °C maximum and only seen between the initial heating run and subsequent cooling run. The activities for this gas mixture increase when increasing the platinum loading.

When exposed to a 2:1 O_2/CH_4 mixture (4000 ppm methane), the catalysts showed similar behavior. A sudden increase was found on the reaction conversion plots of all catalysts when reaching the same conversion level (ca. 15%), which leads to complete combustion for methane at 475 °C (for all except the 0.5% Pt catalyst). This sudden increase is called light-off effect. Also, a hysteresis could be seen between the two heating runs and between heating and cooling, which is contrast to the results of catalysts exposed to the 5:1 O_2/CH_4 mixture.

When exposed to an O_2/CH_4 ratio of 1:1 mixture (6000 ppm methane), light-off was

observed as opposed to the 2:1 ratio. A hysteresis appeared on the conversion plots between the heating and cooling curves. The light-off effect happened at a given conversion level of ca. 3% for all the catalysts, and all catalysts reached 100% conversion at 550 °C.

From the results of changing the gas composition above, it's obvious that on going from fuel lean to fuel rich mixture, the catalysts become more activate at a given temperature. Light-off effect helps with the increasing activities. When the temperature below the light-off point, methane conversion under fuel rich condition is still higher.

Comparing conversions on 4% Pd/Al_2O_3 and Pt/Al_2O_3 catalysts, it's obvious that under 5:1 oxygen-methane ratio (fuel lean condition), the platinum catalyst behavior is worse than palladium catalyst. Pt catalyst exhibits 1.2% conversion at 300 °C, while Pd catalyst shows 23% conversion at the same temperature. With palladium catalyst, methane conversion reaches 100% at only 450 °C. In contrast, the platinum catalyst only shows 93.8% methane conversion at 550 °C (the highest temperature in this reaction).

When the gas mixture ratio is 1:1 (fuel rich condition), the result is completely different. Going from 350 °C to 375 °C, the methane conversion on platinum catalyst changes from 4.0% to 59.0%, while for palladium catalyst, the conversion only changed from 33.0% to 50.7%. This rapid increasing of activity is called light-off. After the light-off point, the methane conversion on platinum catalysts is higher than that on palladium catalyst.

Before the light-off point, the platinum catalyst is more active under fuel rich condition. This indicates that oxidation for the platinum surface would reduce the activity. Hicks et al [28] studied in this area and found that dispersed platinum which forms PtO_2 when oxidized is much less active than larger crystallites with a chemisorbed oxygen layer.

For palladium catalysts, palladium is more active under fuel lean condition due to metal palladium adsorbs oxygen more strongly than the oxidized palladium. Therefore, when tested under fuel lean conditions, palladium catalyst is superior. Also before the light-off point under all fuel rich conditions, palladium catalysts is more active than platinum.

2.6 Light-off phenomenon

The light-off feature is observed on the platinum catalysts under both stoichiometric and methane rich conditions [36]. Cullis and Willatt [24] and Trimm and Lam [37] also observed similar jump in activity for platinum catalysts. There are several possible explanations for that.

One possibility is local heating. Since methane combustion is an exothermic reaction, the metal particles on surface area would have a relatively higher temperature due to the heat generation. Some studies have been done to measure the temperature difference between the support and the metal particles. Some found the temperature difference up to 190 °C [38], while others found little temperature difference [39]. A rapid dissipation of heat transferred from metal particles to the support may cause the little temperature change.

This local heating effect could explain the light-off feature. The metal particle areas are hotter than the support, then the energy barrier for methane oxidation could be overcame easier. But the reason why the light-off effect occurs only at certain conversion instead of a specific temperature was still not clear. In the study of Burch and Loader [36], a ca. 15% for the stoichiometric mix and ca. 3% for the fuel rich mix are observed, while no light-off effect is seen under fuel lean condition. Therefore, the total amount of heat generated on the metal particles could not explain the light-off phenomenon itself. Instead, it is possible that certain concentrations of adsorbed methane and oxygen on the surface would favor the methane combustion [40]. Also, since the methane combustion is first order to methane and zero order in oxygen, the methane molecular approach and dissociative adsorption might play an important role. Therefore, optimum fractional coverage of the surface by both reactants is a requirement for light-off effect. That could explain the difference of platinum catalyst behavior under fuel lean, stoichiometric and fuel rich respectively: too much oxygen present at all conversions leading to no enough methane adsorbed on the catalyst for fuel lean conditions, which would inhibit the light-off effect, and other two gas mixtures have enough present for both reactants. Surface coverage by adsorbed species is another effect for light-off phenomenon.

In contrast to platinum catalyst, there is no light-off effect observed on the palladium catalyst. It might be because palladium adsorbs too much oxygen and could not meet the surface coverage requirement for light-off effect.

2.7 Bimetallic catalysts

As shown above, monometallic palladium and platinum catalysts show high activities in methane combustion, but affected by a different degree in terms of metal/oxide surface ratio, that affects the catalytic performance. For example, at about 700-800 °C, the palladium oxide decomposes to metallic palladium, and palladium oxide is reformed after cooling down. It shows that the catalyst performance is not stable [41]–[43]. Palladium catalysts also have a low resistance of poisoning, which is also a big problem. The addition of a second metal might enhance the activity of palladium or platinum catalysts.

For example, in 1993, Tatsumi Ishihara et al [44] found that adding some metal oxides enhances the activity of Pd catalyst. The suggested mechanism is that the metal oxide additions enhance the oxidation activity of Pd, which is rate determine step of catalyst performance. In their experiments, alumina supported Pd catalysts with several metal oxide additives were tested and studied, such as NiO, SnO_2, Ag_2O, RhO and so on. With the help of X-ray diffraction, they found that Pd was highly dispersed and the difference in each catalyst's dispersion was small. Thus, the observed activity enhancement was not due to improved Pd dispersion, but because metal oxide additives adsorb gaseous oxygen molecules, dissociates them to atomic oxygen, and then provide them to Pd. The oxygen concentration improved by additives was also reported by T. Furuya et al [45].

In the catalyst materials that have been tested in the study by K. Persson et al [43], the bimetallic catalysts can be divided into three types, depending on how the co-metal interacts with the support and/or the palladium. 1). The co-metal reacts with the alumina support to form a spinel phase (for example, for Co and Ni additives), 2) the co-metal forms separate particles (Rh, Ir, Cu, Ag), 3) the co-metal alloys with Pd: PdPt and PdAu. The same types of the co-metals

usually have similar properties. The found activity trend was: Pd > PdNi > PdCo > PdRh > PdAg > PdPt > PdIr > PdAu > PdCu. Co-metals forming a spinel structure (PdCo and PdNi) do not improve the activity stability of palladium catalysts. The spinel structure improves the thermal stability of the support materials. Co-metals forming separate particles (PdRh, PdIr, PdCu, and PdAg) may improve the stability, depending on whether the co-metals are in close contact with Pd. PdRh didn't improve the catalytic activity [46], [47]. PdCu improved the resistance to sulfur [48], PdAg showed improved stability, as well as co-metals forming an alloy with Pd (PdPt and PdAu).

Some works address addition of platinum to palladium for improved methane combustion [49]. In the study by Y. Deng and T.G. Nevell [50], the activity of a catalyst which has 7.5 wt.% Pd and 7.5 wt.% Pt supported on Al_2O_3 was lower on heating than the palladium catalyst with the same metal loading. During the hearing, the temperature is 20 °C lower than the reference catalyst at the same 50% conversion point. While cooling from full conversion, the bimetallic catalyst showed 50% conversion at 30 °C lower temperature than the reference catalyst.

The reasons of better performance for Pd-Pt bimetallic catalyst have been studied [51]. The Pt-Pd bimetallic catalyst was compared to monometallic Pt and Pd catalysts. The three different kinds of catalysts were prepared on alumina support with the same method. After comparing the activity of these three catalysts, they found that the Pd catalyst supported on Al_2O_3 deactivated quickly and after about 15 hours, conversion below 10% was obtained. The Pt catalyst, which has the lowest activity in the beginning, showed about 20% conversion after a long period of reaction. The Pt-Pd bimetallic catalyst, after initial deactivation, showed 50% conversion constantly.

The experiments above showed Pt-Pd bimetallic catalysts have a higher durability than the other two. This is thought to be attributed by the platinum which inhibits sintering of Pd/PdO.

K. Narui et al [52] observed the same improvement of Pt-Pd bimetallic catalysts durability. The Pt added to PdO prevented the deactivation and increased the activity (from 90% to 98% conversion at 350 °C) (Fig 2.9) according to the results.

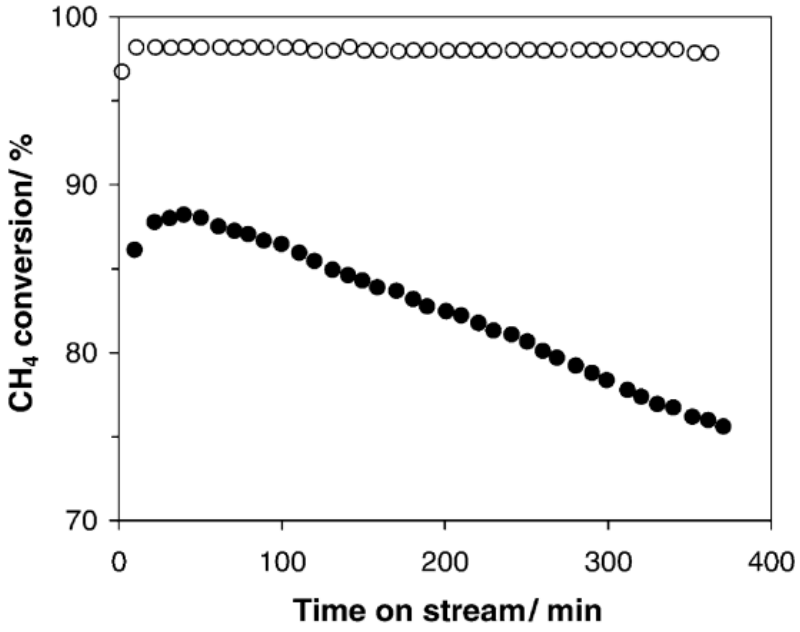

Fig. 2.9. Methane conversion at 350 °C: Black spheres, 0.5 wt.% Pd supported on α-Al_2O_3; White spheres, 0.5 wt.% Pd-0.1 wt.% Pt supported on α-Al_2O_3. Reprinted with permission from [52].

The improvement attributed to Pt is because of the higher dispersion of the catalyst particles and the suppression of the particle growth in the presence of reactants on the basis of ex situ observation of catalysts by transmission electron microscopy. From measurements, it was observed that the PdO particles migrated and coalesced with each other between 570 °C to 590 °C, which was not observed on Pt-Pd metallic catalyst sample. The study of C. Micheaud et al [53] agrees with that of K. Narui et al [52].

In general, in high-temperature applications, especially in the presence of oxygen and or steam, sintering is one of the main reasons that cause the loss of catalyst activity. Mechanism of sintering details has been studied by Tyne Johns et al [54]. In their study, they found a way to detect the atom emission from nanoparticles by observing the same region of the sample under rapid short-term heating conditions. First-principle density functional theory (DFT) calculations were used to show the barrier of atom emission.

In their research, under air conditions, monometallic Pd was found to be stable and hardly sinter at < 800 °C with atmospheric pressure. This is because of the rapid formation of bulk PdO transformed from Pd, which would stop the adatoms from emission to vapor phase. Only limited amount of sintering happened at the early stages of oxidation. In contrast, under air condition, monometallic Pt sinters rapid. Pt have high vapor pressure in the presence of air. When temperature gets higher than 800 °C, significant transport of Pt atoms emitted to vapor phase and reform large particles on the surface. But under reducing conditions, monometallic Pd sinters more than monometallic Pt.

For the bimetallic Pt-Pd catalyst, with the formation of Pt-Pd alloy, Pd lowers the rate of Pt atoms emission to vapor phase. PdO does not help slowing the Pt emission rate because there is no PdO surface shell observed on the bimetallic particles. Therefore, it is Pd that slows the Pt sintering in bimetallic Pt-Pd catalysts. Also, Pt helps Pd keeping in metallic form on the particles surface. However, when the temperature gets significantly high, the Pd has a different role. When heated at 750 °C and 800 °C for 1.5 hours, a rapid Pt loss was observed. The loss of Pt metal is caused by evaporation. Diffusion of adatoms is significant at lower temperature and vapor phase transport becomes more important only at high temperature.

DFT calculations could explain the results. For monometallic Pt, the emission of Pt as PtO_2 to the vapor phase has an energy barrier of 1.7 eV, while that of emission to the support has a much lower harrier as 0.9 eV. For monometallic Pd, the emission energy of PdO to the vapor phase is 4.2 eV. Therefore, there is no expectation of PdO emitted to the vapor phase.

For the Pt-Pd catalysts, the detachment energy for Pt emitted to vapor phase as PtO_2 is 1.6 eV, slightly lower than in the monometallic Pt. With the similar detachment energy for Pt in monometallic Pt and bimetallic Pt-Pd catalysts, it could be explained the rapid particle size growth. Pd does not stop the process of particle growth in the bimetallic catalysts. Also, the bimetallic Pt-Pd stays metallic, which means the presence of Pt would keep the Pd in metallic phase.

This particular insight study [54] was just published in August 2015, and many questions

still remain, such as the particle size and water effect on the volatilization processes.

3. Challenges in the field and the work objectives

As mentioned in the literature review, catalytic heaters face a number of problems, such as unsteady temperature and reactant profiles, incomplete methane combustion, catalyst deactivation and inhibition by produced water. Several studies showed that the use of bimetallic Pd-Pt catalysts may improve performance in methane combustion versus monometallic catalysts. However, most of the studies use powdered alumina support for the Pd or Pt particle deposition, resulting 2-20 nm particle size. The powdered alumina cannot be directly used for heaters because of low mechanical stability and high pressure drop if the alumina powder is wash coated on pads used for heaters. There is a gap in catalyst knowledge if the metal is deposited directly on pads. Moreover, many studies lack comparison of catalyst performance at different methane-to-oxygen ratio and most of them are conducted in the very low water presence (only generated water), which is a known poison.

Thus, the presented study aims to bridge the materials gap between the known Pt-Pd catalysts developed on powdered support for steady-state methane combustion and the commercial pads for combustion at various methane-to-oxygen ratios. The practical target is to decrease the price of the current Pt pads by replacing part of the metal with less expensive palladium, hopefully, not inhibiting the combustion activity.

We selected one metal loading (unless stated otherwise) as typically used in commercial catalytic pads for heaters (0.15 wt. % Pt or Pd or both Pt and Pd) and prepared the catalysts using commercially available metal-free pads. The methane combustion tests were performed in the presence of 5 % water and at two different methane-to-oxygen molar ratios (0.2 and 0.02). Note that in the thesis these conditions are referred as “fuel-rich” and “fuel-lean”, respectively (only in respect to one another), but strictly speaking from the reaction stoichiometry (0.5), both conditions are fuel-lean.

4. Experiments and procedures

4.1 Methane combustion setup and procedure

Methane combustion was performed according to the standard protocols and a flow setup developed previously by Dr. Hayes' group [55].

Fig. 4.1 shows the methane combustion reactor schematic. The reactor is made of an inner tube and an outer sleeve, which is enclosed by a furnace. The inner tube of 3/8" internal diameter and the outer sleeve of 1 inch outer diameter (5/16" inch thickness) are made of 316 stainless steel. This structure is designed to provide efficient heat transfer from the furnace to the tubular reactor as compared to the heat transfer through air. Other details on the setup can be found elsewhere [55]. The reactor tube was put inside of a thick steel casing to help maintain an isothermal reactor. Gas mixture comes into the reactor from the right side, flow through the reactor and flow into GC to get analyzed.

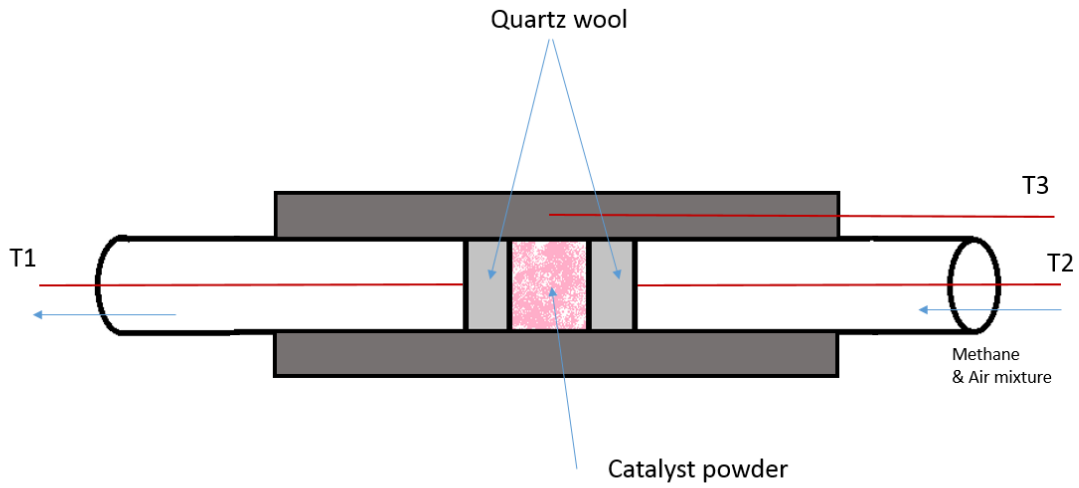

Fig. 4.1. Reactor schematic (T: thermocouple).

Table 4.1 Parameters for methane combustion

Catalyst amount, g	2.14
Gas mixture:	
Methane	8.5 ml/min, 10% balanced in nitrogen
2% oxygen	205 ml/min, 2% oxygen balanced in nitrogen
Air	205 ml/min, extra dry
Reaction:	
Pressure, psi	27
Temperature range, °C	200-650
Water presence, vol. %	5

The reactor was packed with 2.14 g of a calcined catalyst (16 h in static air at 550 °C) that was kept in place by two pieces of quartz wool on each end of the catalyst bed. Methane (8.5 ml/min, 10% balanced in nitrogen, Praxair) was pre-mixed with air (205 ml/min, extra dry, Praxair) or with 2% oxygen balanced in nitrogen (205 ml/min, 2% O_2/N_2, Praxair) to simulate fuel-rich or fuel-lean operating conditions, respectively. The final gas mixture was fed into the catalytic system with a CH_4 concentration of 4000 ppm. There are two mass flow controllers equipped in the methane combustion system to control the methane and air (or 2% O_2/N_2) flow rates. A Mathenson Modular DYNA-blender model 8250 is used for the extra dry air (or 2% O_2/N_2) control. The MKS Type 1479 is used for methane and nitrogen mixture control.

The three thermocouples shown in Fig. 4.1 are K-type thermocouples (Omega). Thermocouples, T_1 and T_2, are used for monitoring the reaction temperature on each end of the catalyst bed. Thermocouple, T_3, monitors and controls the furnace temperature, which is placed in the outer sleeve of the reactor.

Methane combustion was operated at a constant pressure of 27 psi and 200 °C– 650 °C temperature range, with the presence of 5 vol. % water. Water was pumped into the reaction system by a Series II Pump (0.009 ml/min, 0.001 – 5.0 mL/min pump head, self-flush, pulse damper, microstepping, Scientific System Inc.).The water feed was preheated to 150 °C before

feeding into the reactor to prevent condensation.

The whole process for methane combustion has 4 stages: First and second ignition and extinction (without and with 5 vol. % water, respectively) for pre-conditioning the catalysts, hydrothermal aging for catalyst stability test, and third ignition and extinction with 5 vol. % water to evaluate the activity of aged catalysts.

For ignition (I) tests, the temperature was increased from 200 °C to 650 °C stepwise by 50 °C with a ramping rate of 60 °C/min, and held for half an hour at each temperature. The extinction (E) was performed vice versa from 650 °C to 200 °C to study the catalytic performance during cooling down. The catalytic activity was evaluated during ignition and extinction.

The hydrothermal aging (HTA) was conducted in the presence of 5 vol. % water. The reaction temperature was increased to 650 °C and then cooled to a certain temperature used for comparison purposes; the reaction temperature was held for 1 hour at each temperature stage. This high-low temperature cycle was repeated for 8 times. After that the reactor was held at the selected low temperature for 16 hours.

The reactor exhaust was analyzed online every 15 min with an Agilent HP-7890-A gas chromatograph (GC) (Agilent Technologies Incorporation) equipped with series thermal conductivity detector (TCD) and flame ionized detector (FID) for analyzing the compositions of CH_4 and CO_2, respectively. The GC column is a HP-PLOT/Q column of 50 m length, 0.53 mm inside diameter and 40 μm film thickness. Initially the oven temperature was stabilized at 40 °C for 2 min; and then it started to increase at a ramping rate of 50 °C/min until the temperature reached 250 °C and maintained at 250 °C for 1.5 min. Injector and FID temperatures were 200 °C and 275 °C, respectively. Air, hydrogen and helium flow rates were constant at 400, 35, and 25 ml/min, respectively. The split ratio is 5.

The LabView program is used to control and/or monitor the gas flow rates, reaction temperature and pressure, and to communicate with Agilent ChemStation for GC data acquisition.

4.2 Catalyst preparation

The catalyst support (pad Fiberfrax® Durablanket® S) was purchased from Unifrax. The information on the pad provided by the supplier is shown in Table 4.2.

Table 4.2. Technical characteristics of the Durablanket S [56]

Typical Chemical Analysis (wt. %)	
SiO_2	53.0 - 58.0
Al_2O_3	42.0 - 47.0
Alkalis	<0.25
$Fe_2O_3 + TiO_2$	<0.2
Physical Properties	
Color	White
Classification Temperature (°C)	1250
Melting Point (°C)	1760
Mean Fibre Diameter (microns)	3.25
Specific Heat at 1000° C (J/kgK)	1140
Thickness (mm)	12.7
Permanent Linear Shrinkage (%) 24 hour soak	
1250 °C	2.6
Density (kg/m^3)	128
Thermal Conductivity (W/mK)	
Mean Temp.	
600 °C	0.12
800 °C	0.18
1000 °C	0.28
Tensile Strength (kPa)	75

For the catalyst preparation and investigation, the pad was ground to the powdered form. The powder size is around 100 μm after grinding. For the catalyst preparation, the pad was impregnated with a Pt precursor to obtain 0.15 wt. % final Pt loading. This loading was selected to simulate the commercial pads sold in heaters. The catalyst preparation method is dry impregnation. In Table 4.3, different amount of solutions and deionized water used for catalysts preparations is listed.

Table 4.3 Amount of solutions and deionized water used for catalyst preparations

Catalysts	**Pd**	**Pt**	**$Pt_{2.7}Pd$**	**Pt_5Pd**	**Pt_5Pd**	**$Pt_{1.6}Pd$**	**$Pt_{1.6}Pd$**	**$Pt_{1.6}Pd$**
Metal loading, wt.%	0.150	0.150	0.150	0.150	0.075	0.075	0.150	0.300
$PdCl_2$, μl	125.00	0.00	20.80	12.30	6.15	13.75	27.50	55.00
H_2PtCl_6, μl	0.00	98.70	82.20	89.00	44.50	37.00	74.00	148.00
H_2O, μl	475.00	501.30	497.00	498.70	549.35	549.25	498.50	397.00

The preparation steps for an exemplary monometallic palladium catalyst are as follows (micropipette is used for measurements where appropriate):

1. Prepare a precursor solution by mixing 125.0 μl $PdCl_2$ ($PdCl_2$, 5% w/v solution, Arcos) and 475 μl H_2O (deionized water).

2. Immerse 2.5 g of the ground pad into the solution and stir to achieve uniform wetting.

3. Dry in static air in an oven at 60 °C.

Monometallic Pt catalysts were prepared in the same way with aqueous H_2PtCl_6 (H_2PtCl_6, 8 wt. % solution, Sigma - Aldrich) solution. Bimetallic PtPd catalysts were prepared using the same method when mixing the aqueous solution of $PdCl_2$ and H_2PtCl_6 listed in Table 4.3.

The as-synthesized catalysts were stored for no longer than 3 days without special

precautions. Before the catalytic reactions, catalysts were calcined in air for 16 h at 550 ºC to transform the metal precursor to the metal oxide nanoparticles and "de-green" the pad. The calcined catalysts were tested in reactions within 2 days after calcination.

4.3 Catalyst characterization

4.3.1 CO chemisorption

CO chemisorption experiments were performed to estimate the metal diameters for monometallic Pt, Pd and bimetallic $Pt_{1.6}Pd$ catalysts with the same 0.15 wt.% metal loading. These catalysts were calcined at 550 °C for 16 h in furnace in air condition. The calcined samples (1 g) were packed in a quartz U-tube reactor and then loaded to an AutoChem II 2920 Chemisorption Analyzer. Before CO chemisorption, catalysts were reduced in a flow of 10% H_2/Ar (25 mL/min) gas mixture at 650 °C for 16 h, followed by purging in Ar for 30 min and cooled to room temperature in Ar. The in situ hydrogen reduction and inert treatment provided clean metallic surfaces for the following CO chemisorption. CO chemisorption experiments were performed by dosing 3% CO/H_2 gas mixture at room temperature. The volumetric flow rates of 3% CO/He loop gas and the He carrier gas were 25 mL/min. Nanoparticle dispersions were calculated by assuming stoichiometry of 1.

4.3.2 Transmission electron microscopy (TEM)

The TEM analysis of supported catalysts was performed using a JEOL 2100 transmission electron microscope operated at 200 kV. The calcined (at 550 ºC for 16 h) Pt, Pd and bimetallic $Pt_{1.5}Pd$ pads were dispersed in ethanol by sonicating for 5 min. Samples for TEM were prepared by placing a drop of the suspension onto a carbon-coated copper grid, followed by evaporating the solvent in a 60 °C oven for overnight. Mean diameter and standard deviation of more than 150 particles were determined using ImageJ software. Linear diameter was used for the

evaluation.

4.3.3 Temperature-programmed reduction (TPR)

The TPR of the pre-calcined catalysts were performed with H_2/Ar gas mixture using an AutoChem II Chemisorption Analyzer (Micromeritics, USA) equipped with a thermal conductivity detector (TCD). A series of oxidation-reduction-oxidation-reduction experiments were performed, with final reduction profiles recorded and reported. Prior to TPR analysis, catalysts were calcined at 550 °C for 16 h. The calcined catalysts (1g) were loaded in a quartz U-tube reactor. The calcined catalysts were reduced in a flow of 10% H_2/Ar (25 mL/min) at 650 °C (highest temperature for catalyst test) for 30 min. After the calcination-reduction pretreatment, samples were purged with Ar for 30 min at 650 °C and cooled down to room temperature in Ar. The catalysts were then oxidized in 10% O_2/He (25 mL/min) at 650 °C for 30 min and then purged with He for 30 min at 650 °C and cooled to room temperature in He. This oxidation was then followed by TPR analysis using 10% H_2/Ar from room temperature to 650 °C with a temperature ramping rate of 10 °C/min. The TCD signals for the reported TPR profiles were inverted; so positive peaks indicate hydrogen consumption.

5. Results and discussion

5.1 Catalyst characterization

Metal nanoparticle size, as well as bimetallic interactions are known to affect the catalytic behavior of Pt and Pd in methane combustion, as discussed in the literature review. Thus, monometallic Pt, Pd and a representative bimetallic $Pt_{1.6}Pd$ catalyst with 0.15 wt. % loading on the support were analyzed after the pretreatment used in the catalytic reactions (calcination in air at 550 ºC for 16 h) for the nanoparticle size (TEM and CO chemisorption) and bimetallic interactions (TPR).

Fig. 5.1 shows the TPR profiles for the three catalysts. Monometallic Pd exhibits a hydrogen evolution peak below 100 ºC, that is typical for the Pd-hydride decomposition. Pt oxide on the monometallic Pt pad showed a broad hydrogen consumption peak corresponding to the oxide reduction at ~ 500 ºC. The bimetallic catalyst also exhibited the Pt-specific high-temperature reduction peak but did not show the Pd-characteristic hydrogen evolution peak, which implies the Pt-Pd interactions in the bimetallic catalysts.

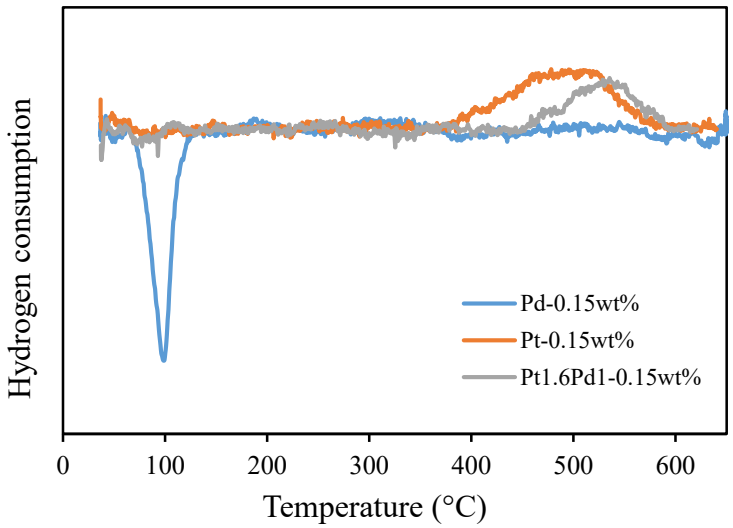

Fig. 5.1. TPR profiles of the representative catalysts pretreated at 550 ºC in air for 16 h

The metal nanoparticle size was evaluated via CO chemisorption of the catalysts calcined at 550 ºC for 16 h followed by reduction in hydrogen at 650 ºC, with the oxidation-reduction cycle performed twice to intensify the catalyst aging. The results in Table 5.1 show evidence that Pt alone undergoes significant sintering, much exceeding the Pd alone. When Pt is diluted with Pd in the bimetallic catalyst, the latter brings improved stability against sintering. Such large particle sizes could be expected given the non-porous nature of the supporting pad.

Similar sintering behavior of Pt, Pd and Pt-Pd catalysts was reported by other groups [54].

Table 5.1. CO chemisorption results and nanoparticle sizes of the calcined and reduced catalysts

Catalyst, 0.15 wt.% loading	Amount of CO adsorbed, μmol CO/ mol metal, s	Nanoparticle diameter assuming CO/metal molar ratio of 1, nm	Dispersion fraction, [-]
Pd	11400	~ 100	0.0114
Pt	2900	~ 400	0.0029
$Pt_{1.6}Pd$	13100	~ 150	0.0131

TEM of the calcined-only catalysts (550 ºC for 16 h, Fig. 5.2 and Table 5.2) show that such “fresh” Pt pad reveals bimodal Pt nanoparticle distribution (3-12 nm Pt nanoparticles with agglomerates above 20 nm). Pd nanoparticles are larger but more uniform, while the bimetallic catalyst shows an intermediate particle size with no large Pt agglomerates as characteristic of monometallic Pt nanoparticles. For all the catalysts, the particle sizes after calcination only (Fig. 5.2) are significantly smaller than after two oxidation-reduction cycles at high temperatures (Table 5.1), which indicates that the single calcination is not sufficient to complete the aging process and some structural changes may happen during high-temperature methane combustion.

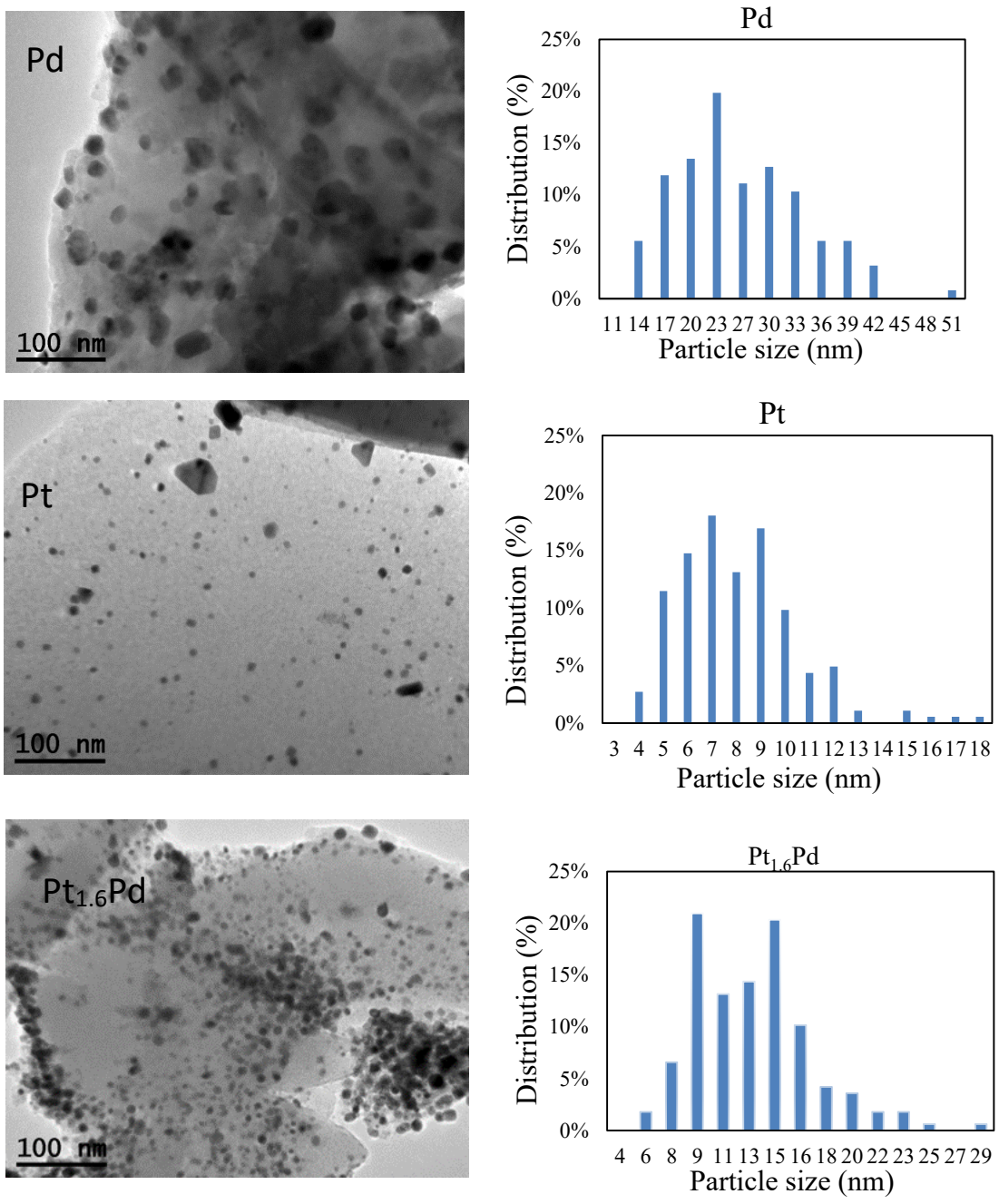

Fig. 5.2. TEM images of calcined selected catalysts and linear size distribution based on diameter of 160+ particles in a sample. The Pt sample also contains unaccounted large 20+ agglomerates

Table 5.2. Data analysts of calcined Pd and Pt catalysts particle sizes

Particle diameter, nm	Pt*	Pd	$Pt_{1.6}Pd$
Average, based on linear distribution for particle diameter, nm	8*	25	12
Maximum, nm	18*	49	25
Minimum, nm	4*	12	5
Standard deviation, nm	3*	8	4

* Pt catalyst also contains unaccounted in this distribution agglomerates of 20+ nm size, and data above was calculated without those agglomerates more than 20+ nm.

5.2. Mass transfer limitations

Mass transfer limitations is an important factor that affects the catalysts activity performance. To make sure that there is no mass transfer limitation, two experiments were conducted using a bimetallic catalyst $Pt_{2.7}Pd$ with total metal loading of 0.3 wt. % at the same WHSV (weight hour space velocity). In the first experiment, 2.1433 g catalyst were used and tested under 8.5 ml/min 10% methane in nitrogen and 204 ml/min 2% oxygen in nitrogen gas mixture. For the second ignition and extinction cycle in which water was added, the water amount was 0.009 ml/min. The second experiment was run under 75% of the previous conditions: feed rate, catalyst amount and water amount. As seen from Fig. 5.3, the same conversion curves were obtained. For example, at 550 °C, the conversions are 87±2% for the first (no H_2O) ignition-extinction curves and 16±1 for the second (with H_2O) ignition extinction curves. Thus, there are no external mass transfer limitations at the tested conditions.

The support pad contains fibers of only 3.25 micron diameter, so the internal diffusion limitations may be excluded.

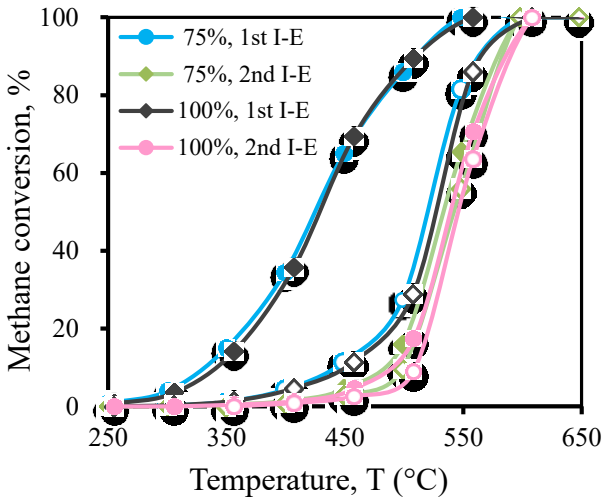

Fig. 5.3. I-E curves for $Pt_{2.7}Pd$ catalyst (0.3 wt. %) to verify external diffusion limitations. Closed symbols indicate ignition (I), open symbols indicate extinction (E)

5.3 Catalyst performance under fuel-rich conditions

5.3.1 Monometallic palladium and platinum catalyst

Monometallic Pt catalyst was prepared with a metal loading of 0.15 wt. % that was the same as in commercial pads for heaters. The same weight loading was used to evaluate the performance of monometallic Pd catalyst. In a typical test, four experimental stages were conducted in a flow reactor with the effluent analyzed to determine methane conversion. In the first ignition (I) - extinction (E) cycle, dry methane/air mixture was fed to the reactor; the reactor was heated to 650 °C and then cooled to 200 °C. 5 vol. % of water was added to the feed when performing the second I-E cycle. After the second I-E, hydrothermal aging (HTA) was conducted to measure catalyst stability for up to 40 hours on stream. The third ignition-extinction was performed after HTA to evaluate the performance of the used catalyst in the presence of water.

The catalytic results for methane combustion on monometallic Pt pad are presented in Fig. 5.4 for methane/oxygen ratio of 0.2 (fuel-rich conditions). Platinum shows insignificant poisoning by water in the feed and the behavior of the used catalyst in the 3rd I-E cycle is similar

to the fresh catalyst. Also, there is almost negligible hysteresis between I and E both in dry and wet conditions, with the catalyst being more active at extinction. Contrary to Pt, Pd was found more active during ignition with a large hysteresis between I and E curves (Fig. 5.5). Pd activity reduced significantly when water was added. HTA and two other I-E cycles were not performed because the catalyst showed incomplete methane combustion even at 650 ºC.

Fig. 5.6 compares the performance of Pt and Pd. Although Pd is more active than Pt in the dry feed, it is more susceptible to water poisoning and shows inferior performance to Pt at the same loading under FR wet conditions. Thus, Pt cannot be fully replaced by Pd.

5.3.2 Bimetallic Pt-Pd catalysts

A variety of Pt-Pd catalysts with different Pt:Pd molar ratios were prepared (Table 5.3) and tested in fuel-rich methane combustion. The same pad amounts (2.14 g) were used to evaluate the catalytic performance. Table 5.4 compares temperatures of 10%, 50% and 100% methane conversion for the ignition-extinction experiments.

Table 5.3. Summary of the bimetallic catalysts studied in fuel-rich methane combustion

	$Pt_{2.7}Pd$	$Pt_{1.6}Pd$	Pt_5Pd	Pt_5Pd	$Pt_{1.6}Pd$
Total metal loading on a pad, wt. %	0.15	0.15	0.15	0.075	0.075
Loading on a pad, wt. %	Pt: 0.125 Pd: 0.025	Pt: 0.1125 Pd: 0.0375	Pt: 0.135 Pd: 0.015	Pt: 0.068 Pd: 0.007	Pt: 0.056 Pd: 0.019
Loading in the reactor, mmol	Pt: 0.0137 Pd: 0.0050	Pt: 0.0124 Pd: 0.0076	Pt: 0.0149 Pd: 0.0030	Pt: 0.0074 Pd: 0.0015	Pt: 0.0062 Pd: 0.0038
Metal(s) price loaded in the reactor, US cents*	15.3	14.5	16.0	8.0	7.2

* based on 6-year average data from 2009 through 2015 from www.nasdaq.com (1,500 USD per once Pt and 650 USD per once Pd). Price of the Pt alone loaded in the reactor is 17.0 US cents

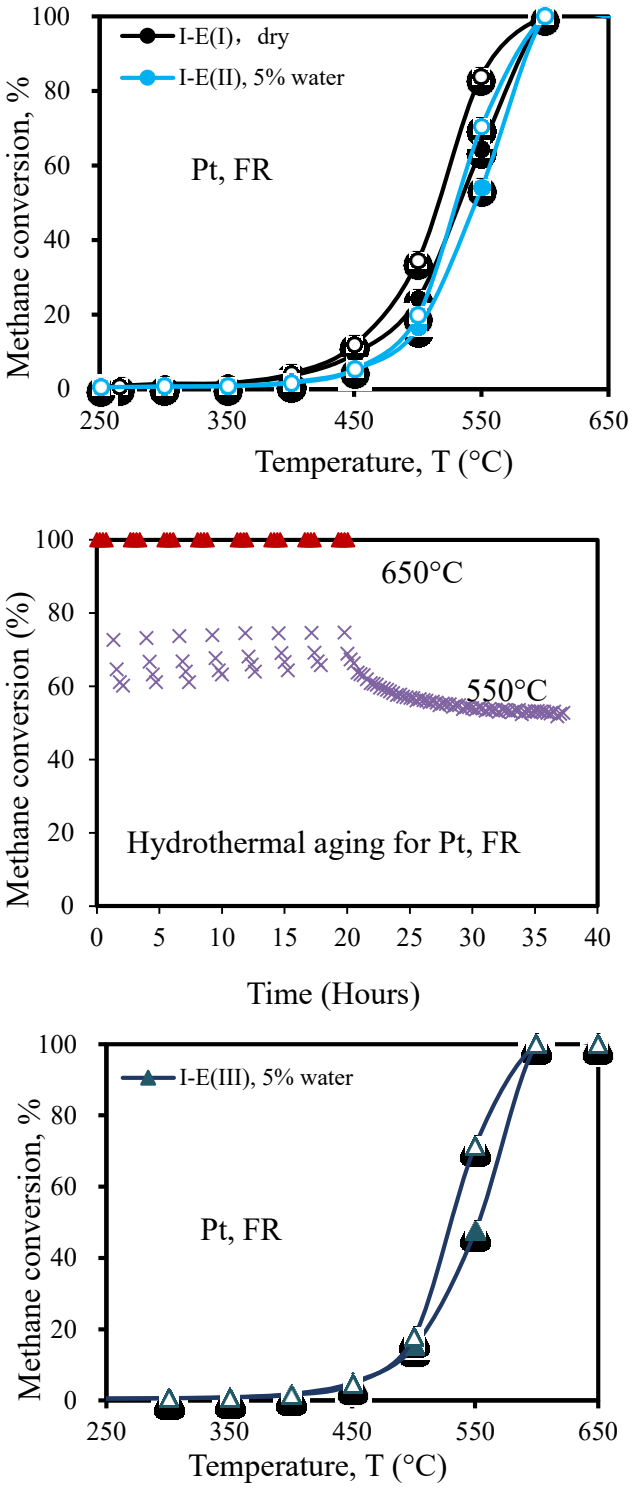

Fig. 5.4. Pt (0.15 wt. %) pad performance in methane combustion under fuel-rich (FR) conditions. Closed symbols indicate ignition (I), open symbols indicate extinction (E)

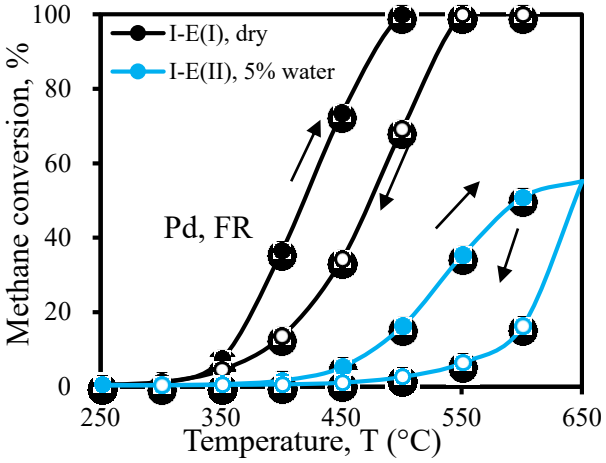

Fig. 5.5. Pd (0.15 wt.%) pad performance in fuel-rich methane combustion

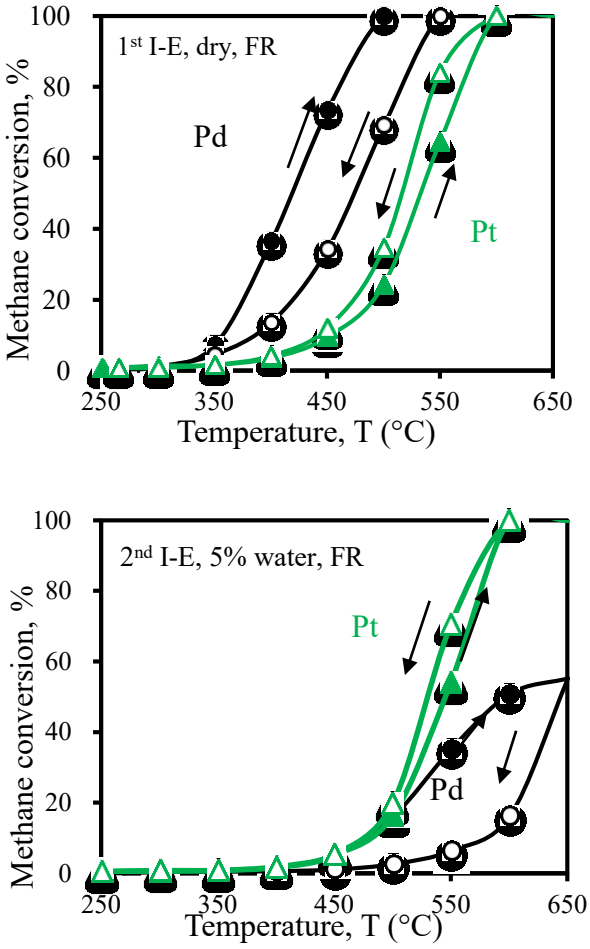

Fig. 5.6. Pd and Pt performance in fuel-rich methane combustion. Closed symbols indicate ignition (I), open symbols indicate extinction (E)

Table 5.4. Temperatures of 10%, 50% and 100% methane conversion under FR conditions

1st I-E	Pd	Pt	$Pt_{2.7}Pd$	Pt_5Pd		$Pt_{1.6}Pd$	
	0.15wt%	0.15wt%	0.15wt%	0.15wt%	0.075wt%	0.075wt%	0.15wt%
First I-E (dry feed)							
$T_{10\%}$(I)	358	452	325	478	490	501	304
$T_{10\%}$(E)	387	443	472	491	500	523	410
$T_{50\%}$(I)	420	532	402	547	563	576	371
$T_{50\%}$(E)	477	517	538	530	548	574	539
$T_{100\%}$(I)	501	600	500	600	600	650	450
$T_{100\%}$(E)	551	600	600	600	650	650	600
Second I-E (5% water)							
$T_{10\%}$(I)	476	482	499	503	515	523	469
$T_{10\%}$(E)	580	475	509	503	512	549	508
$T_{50\%}$(I)	600	546	550	558	570	591	539
$T_{50\%}$(E)	645	530	558	558	566	595	562
$T_{100\%}$(I)	-	600	600	600	650	650	600
$T_{100\%}$(E)	-	600	600	600	650	650	650
Third I-E after HTA (5% water)							
$T_{10\%}$(I)		482	518	518	528	559	511
$T_{10\%}$(E)		468	508	510	519	501	511
$T_{50\%}$(I)		553	575	570	582	619	572
$T_{50\%}$(E)		531	570	560	577	616	572
$T_{100\%}$(I)		600	650	650	650		650
$T_{100\%}$(E)		600	650	650	650		650

The catalytic results of the Pt:Pd molar ratio for the same 0.15 wt. % total metal loading on the pad are shown in Fig. 5.7. When water was added in the feed, in the 2nd I-E cycle the bimetallic catalysts showed superior performance to their monometallic forms but after 40 hours of HTA their behavior approached Pt performance. At the 3rd I-E cycle, any of the bimetallic catalysts may be chosen as an alternative to Pt with insignificant loss of activity: for example, the temperature of 50% conversion for the 2rd ignition on $Pt_{1.6}Pd$ catalyst is 572 ^{o}C versus 553 ^{o}C for the Pt-only catalyst. More importantly, is that the bimetallic catalysts show stable behavior during HTA (stable 40% conversion, as seen from Fig. 5.7), while Pt progressively loses its

activity from 70% to 50% conversion. Among the three bimetallic catalysts, $Pt_{1.6}Pd$ catalyst is the least expensive (~15% less expensive than Pt alone) with satisfactory performance and can be recommended for Pt replacement. The lower Pt:Pd molar ratio was not tested because the catalysts progressively lose their activity upon dilution with Pd.

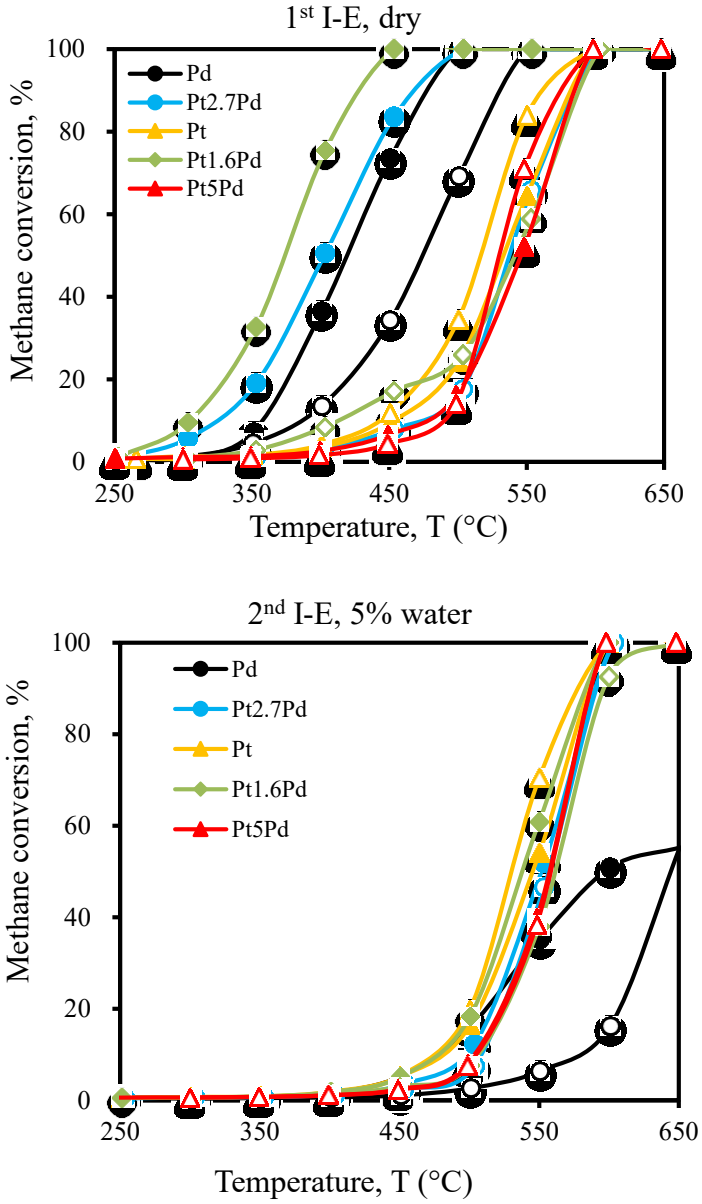

Fig. 5.7.a. 1st and 2nd I-E curves of the bimetallic catalysts with 0.15 wt. % loading under FR conditions. Closed symbols indicate ignition (I), open symbols indicate extinction (E)

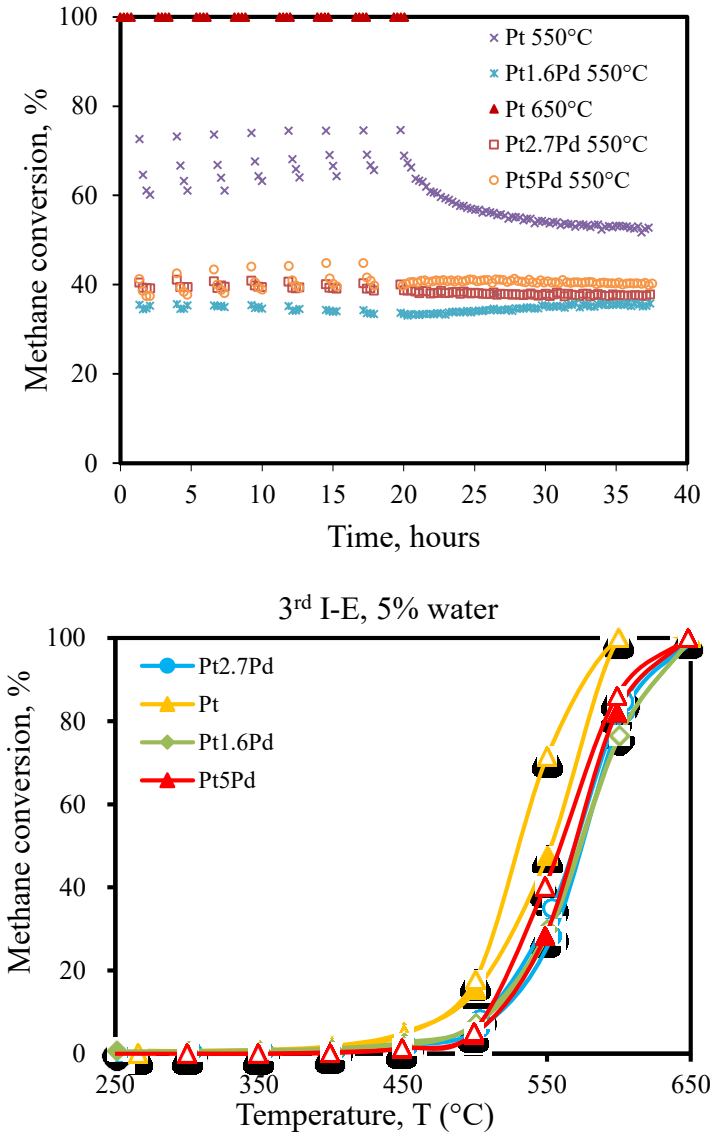

Fig 5.7.b. 3rd and 4th I-E curves of the bimetallic catalysts with 0.15 wt. % loading under FR conditions. Closed symbols indicate ignition (I), open symbols indicate extinction (E)

As was shown in Section 5.1, the nanoparticle size is above 100 nm which corresponds to <1% dispersion. Smaller particles provide higher surface-to-volume ratio, so to increase the number of active sites, a catalyst with lower metal loading (0.075 wt. %) was prepared. Lower metal loading may result in smaller particles.

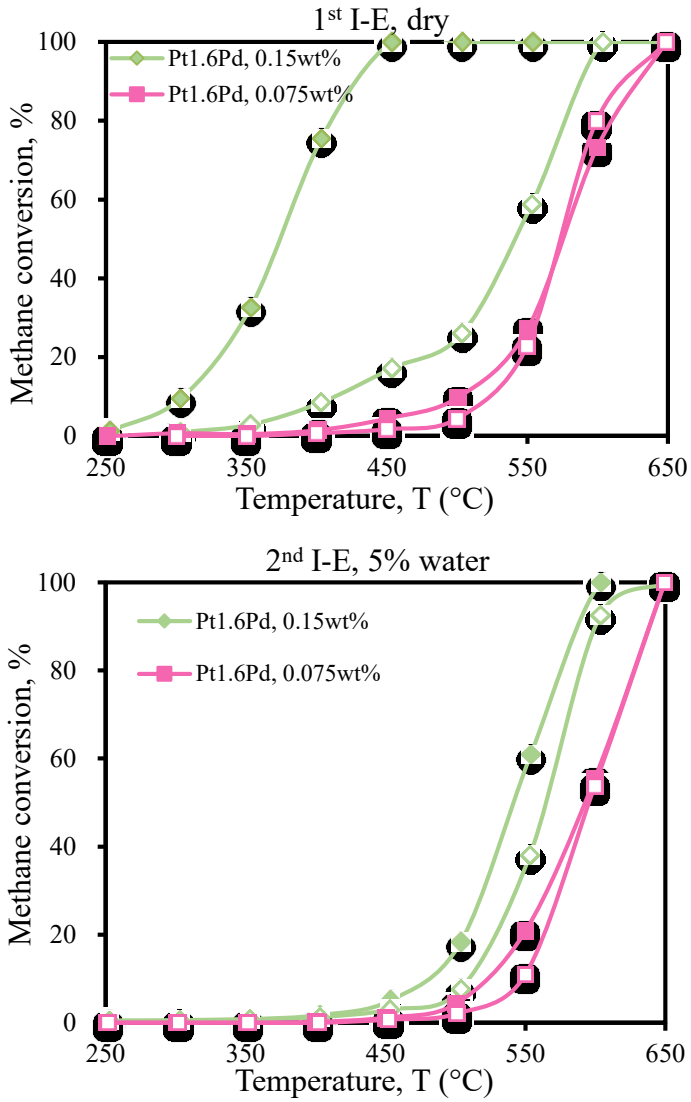

Fig. 5.8.a. 1st and 2nd I-E curves of $Pt_{1.6}Pd$ catalysts with 0.15 wt. % and 0.075 wt. % total metal loading under FR conditions. Closed symbols indicate ignition (I), open symbols indicate extinction (E)

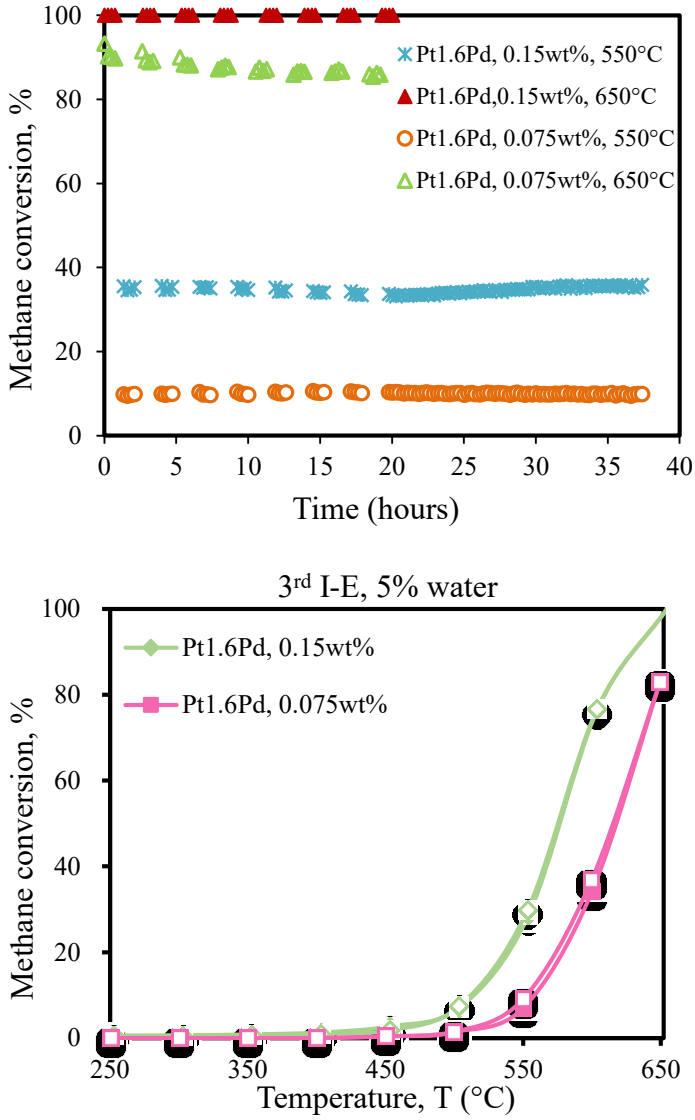

Fig 5.8.b. Thermal aging plot and 3rd I-E curve of $Pt_{1.6}Pd$ catalysts with 0.15 wt. % and 0.075 wt. % total metal loading under FR conditions. Closed symbols indicate ignition (I), open symbols indicate extinction (E)

The lower loading catalyst showed more stable performance from 1st to 3rd I-E cycles, as compared to higher loading catalyst (Fig. 5.8). However, its activity was lower. Most likely, the expected particle size decrease was not enough to offset the double metal loading decrease. Thus, the catalyst with 0.15 wt. % loading is recommended.

5.3.3 Conversion and activity comparison under fuel-rich conditions

To compare all of the catalysts tested under fuel rich condition, several graphs based on the results above are shown in Fig. 5.9 and Fig. 5.10.

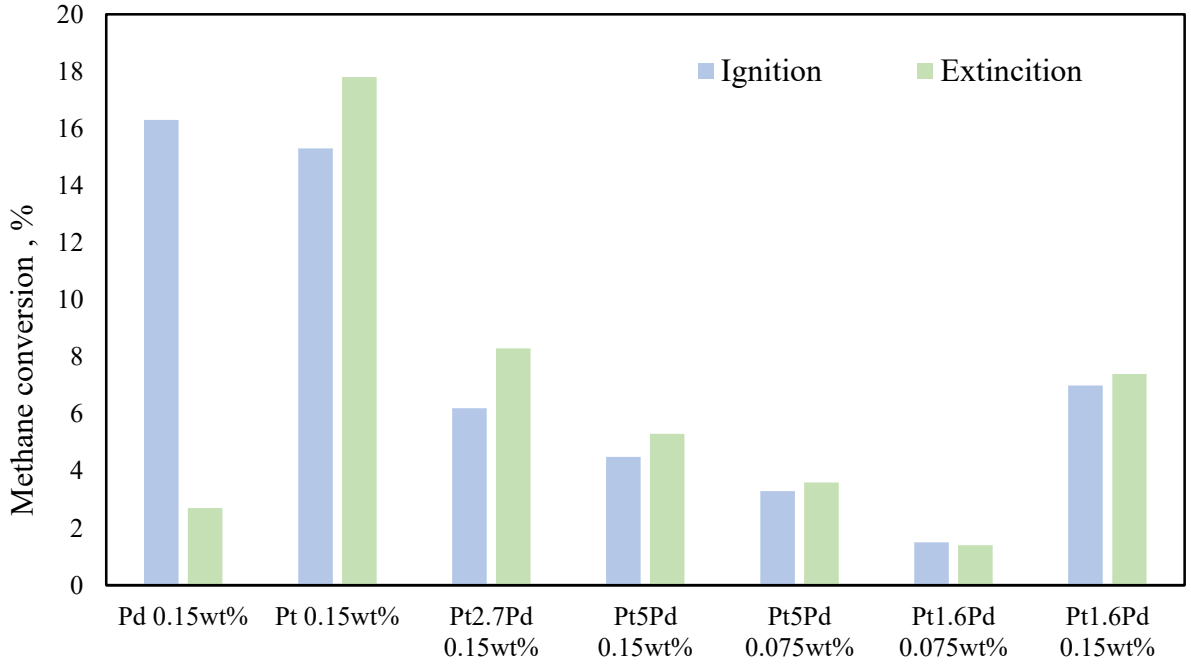

Fig.5.9 Conversions of 3rd I-E for different catalysts under fuel-rich condition. (For monometallic Pd catalyst, the conversion data was from the second I-E curves). The 3rd I-E cycle was tested after hydrothermal aging.

Fig.5.9 shows the conversions for the third I-E (after hydrothermal aging) curve for different catalysts at 500 °C. Among all the catalysts, monometallic platinum has the highest conversions. Monometallic palladium has good conversions in ignition but did poorly in extinction, showing the large hysteresis shown in Fig.5.5. Pt_5Pd 0.075 wt. % & 0.15 wt. % and $Pt_{1.6}Pd$ 0.075 wt. % show lower conversions than $Pt_{1.6}Pd$ 0.15 wt. %. $Pt_{2.7}Pd$ and Pt_5Pd with the same 0.15 wt% total metal loading have similar performance, but the $Pt_{1.6}Pd$ catalyst is the least expensive (Table 5.3).

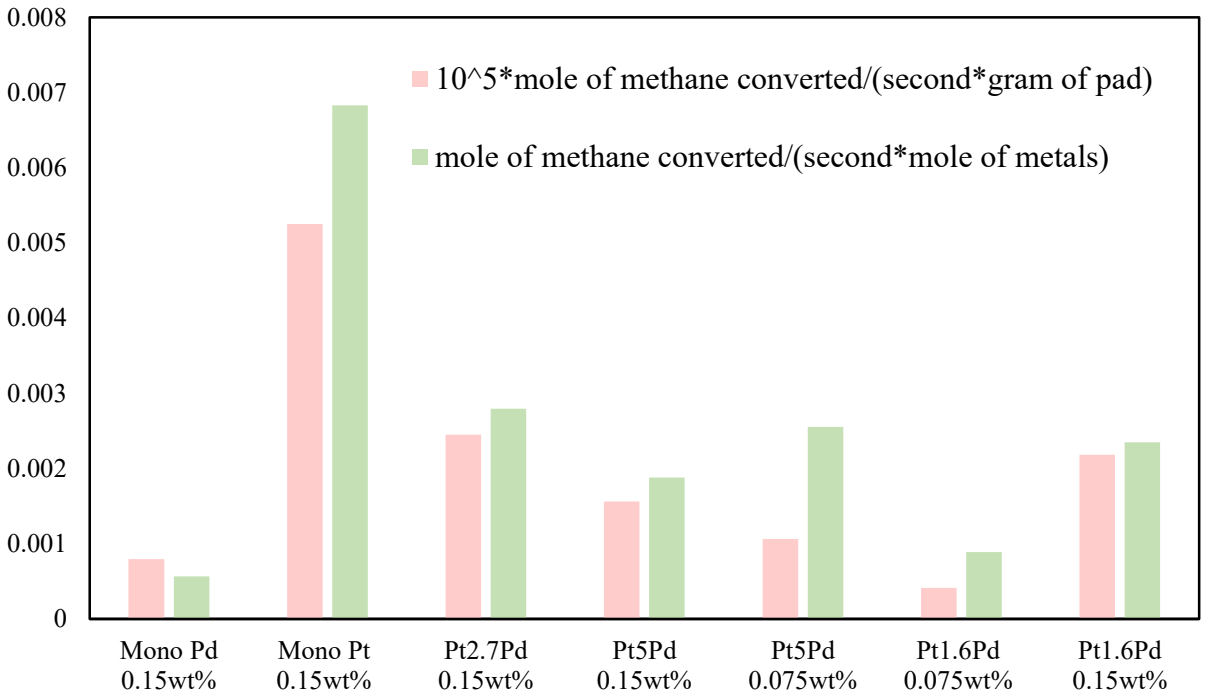

Fig. 5.10. Catalyst activities at 500 °C based on data from Fig. 5.9 (extinction).

Data of Fig. 5. 9 were used to calculate activities presented in Fig. 5.10. All bimetallic catalysts and mono Pd (extinction) in Fig. 5.9 showed <8% conversion and may be closely approximated as a differential reactor activity. These activities may be used to calculate turnover frequency based on CO chemisorption data (Table 5.1). For the Pd-only catalyst, the TOF = 0.0006/0.0114 = 0.053 s^{-1}, for $Pt_{1.6}Pd$ 0.15 wt. %, TOF = 0.0023/0.0131 = 0.176 s^{-1}. The dramatic improvement is attributed not to the particle size, but to the inherent higher activity of Pt-only catalyst under wet FR conditions. TOF calculated for Pt at 550 °C is not possible because of high X (~20%), but the order of magnitude can be estimated as: TOF = 0.0068/0.0023 $\approx$ 2 s^{-1}.

Thus, Pt intrinsically is more active under FR wet conditions than Pd, but Pd is less stable and sinters. Pd addition improves stability and dispersion but lowers the high intrinsic activity of Pt.

5.4 Catalyst performance under fuel-lean conditions and comparison with FR conditions

Based on the results of Chapter 5.3, the best bimetallic catalyst under fuel rich condition is $Pt_{1.6}Pd$ with 0.15 wt. % total metal loading. To test the catalyst behavior under fuel lean condition, monometallic platinum, monometallic palladium and bimetallic $Pt_{1.6}Pd$ with the total metal loading of 0.15 wt. % were prepared and tested for methane/oxygen ratio of 0.02. The same pad amounts were used (2.14 g).

The experimental stages are the same as under fuel rich conditions: first I-E with dry feed, second I-E with 5 vol. % of water added to the feed, hydrothermal aging (HTA) for up to 40 hours on stream, and the third I-E with the presence of water to evaluate the performance of the used catalyst.

The catalytic results for methane combustion of these three catalysts are presented in Fig. 5.11, 5.12 and Table 5.5.

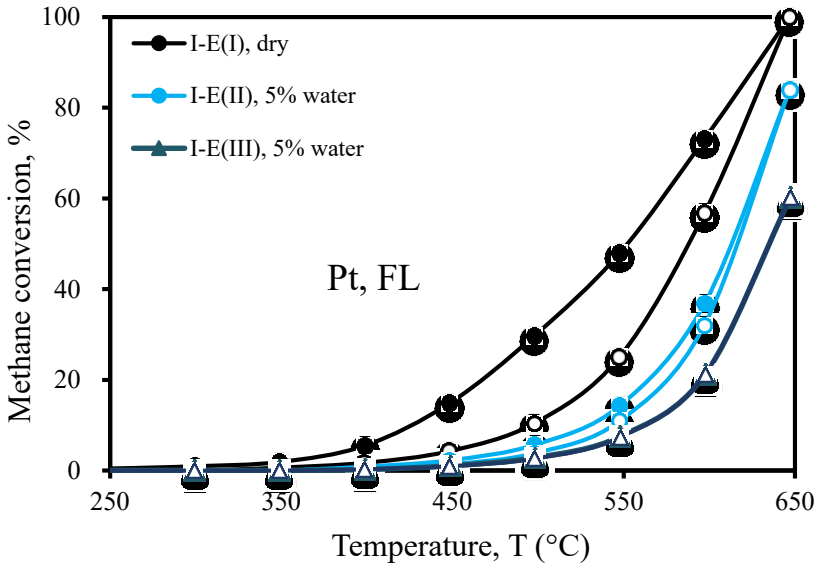

Fig. 5.11.a. Pt pad performance in methane combustion under fuel-lean (FL) conditions. Closed symbols indicate ignition (I), open symbols indicate extinction (E)

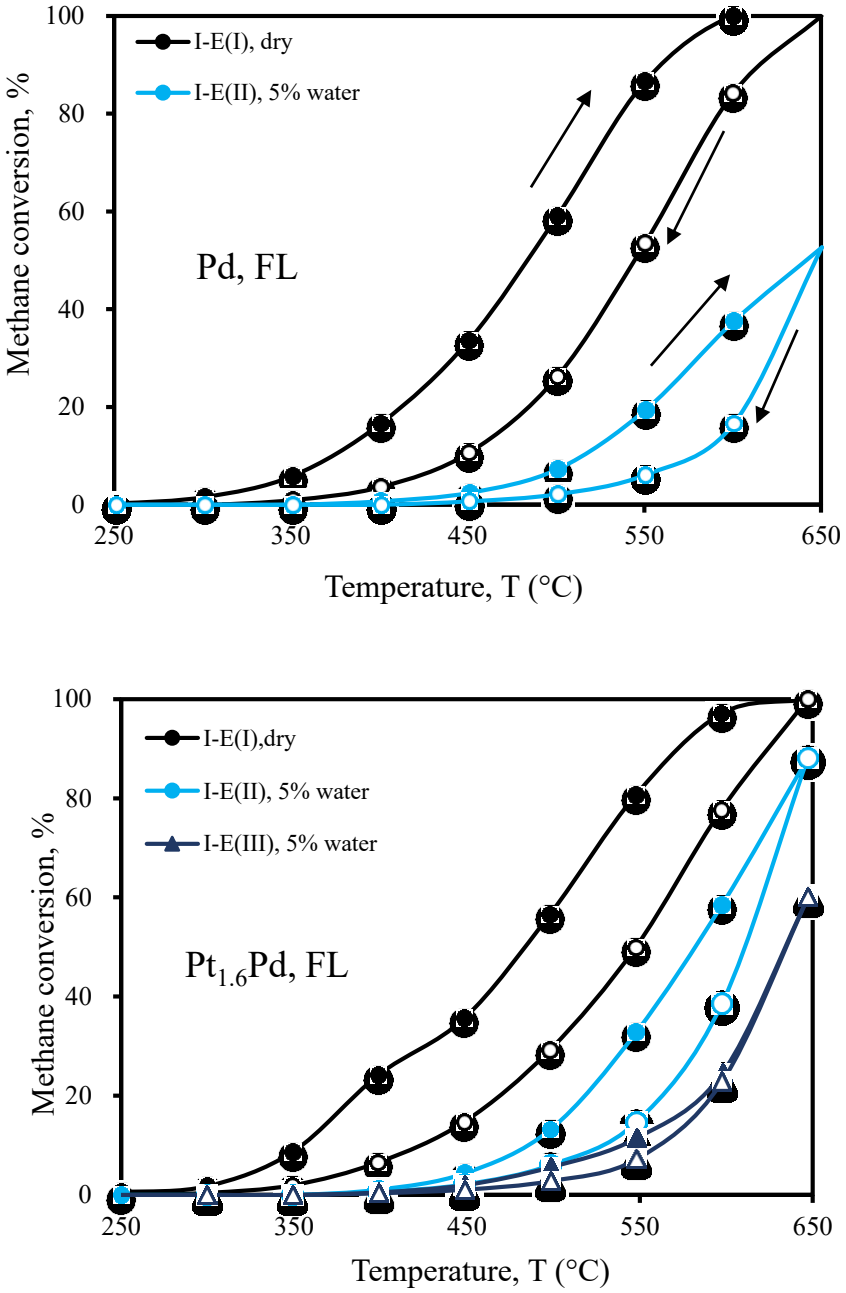

Fig. 5.11.b. Pd and $Pt_{1.6}Pd$ pad performances in methane combustion under fuel-lean (FL) conditions. Closed symbols indicate ignition (I), open symbols indicate extinction (E)

Table 5.5. Temperatures of 10%, 50% and 100% methane conversion under FL conditions

	Pd	Pt	$Pt_{1.6}Pd$	Pd	Pt	$Pt_{1.6}Pd$	Pd	Pt	$Pt_{1.6}Pd$
	First I-E (dry feed)			Second I-E (5% water)			Third I-E (5% water)		
$T_{10\%}$(I)	373	427	355	515	530	485		561	540
$T_{10\%}$(E)	449	495	423	579	543	530		561	560
$T_{50\%}$(I)	484	552	482	641	613	581		635	635
$T_{50\%}$(E)	544	588	548	648	618	610		635	635
$T_{100\%}$(I)	600	650	650						
$T_{100\%}$(E)	650	650	650						

In Fig. 5.11, all of the three catalysts were found more active during ignition than extinction under fuel lean conditions, while under fuel rich condition, Pt was more active in extinction process. Also all the catalysts were poisoned by water added into feed and palladium shows the most significant poisoning by water with a large hysteresis between I and E curves. Pt and $Pt_{1.6}Pd$ have hysteresis in the first I-E curve but in the second and third I-E, the hysteresis is smaller and even negligible. Interesting is that under FR condition (Fig. 5.4) there was negligible difference between 1st, 2nd and 3rd I-E curves for Pt, while under FL condition its performance significantly deteriorated with cycling.

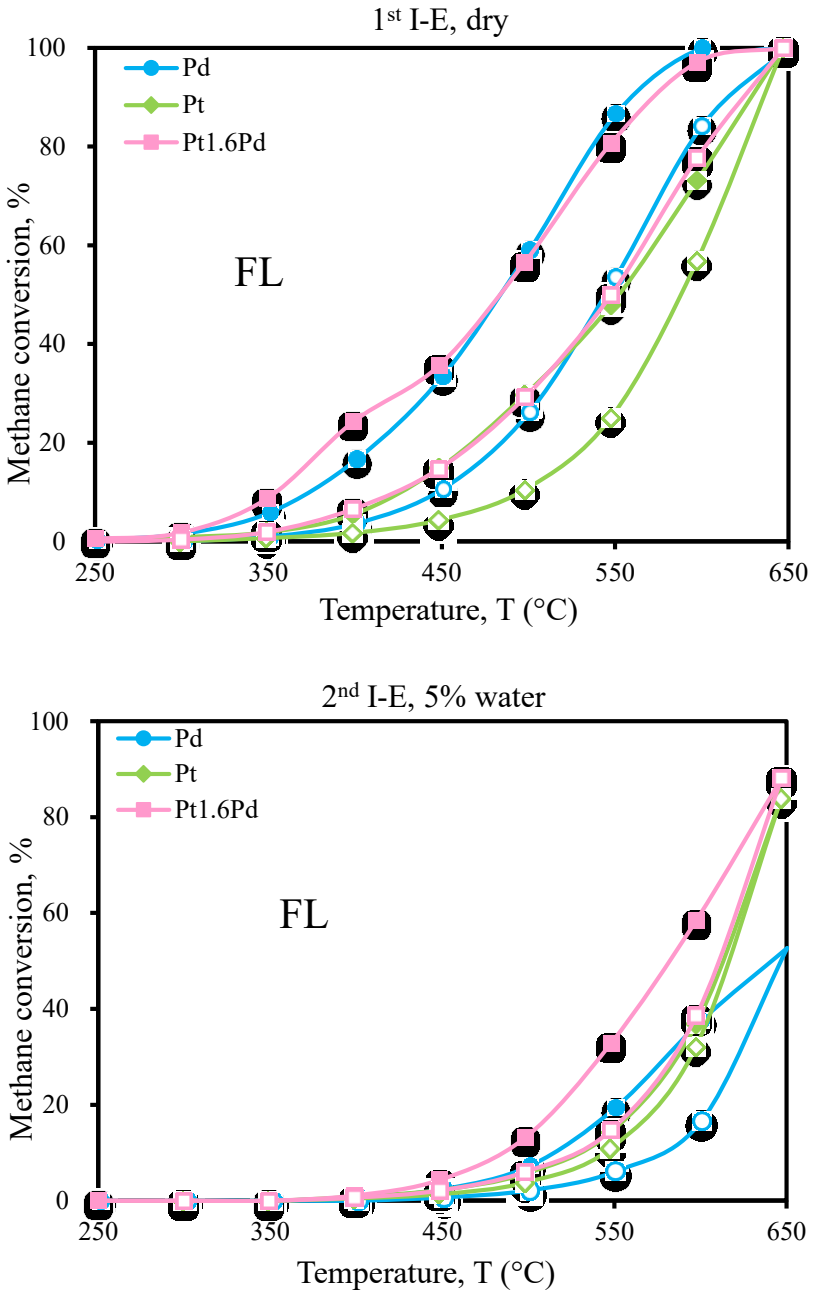

Fig. 5.12.a. 1st and 2nd I-E curves of Pt, Pd and $Pt_{1.6}Pd$ catalysts with 0.15 wt. % loading under FL conditions. Closed symbols indicate ignition (I), open symbols indicate extinction (E)

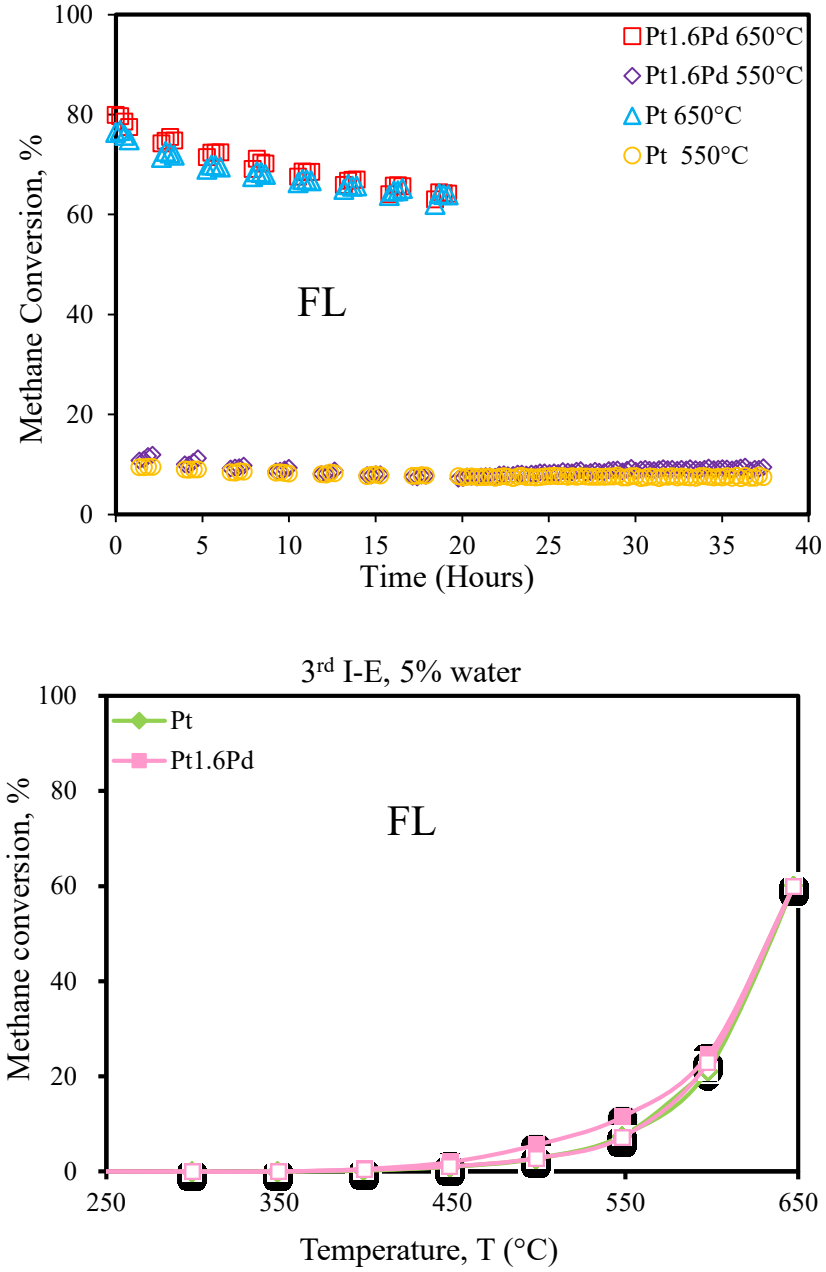

Fig. 5.12.b. 3rd and 4th I-E curves of Pt, Pd and $Pt_{1.6}Pd$ catalysts with 0.15 wt. % loading under FL conditions. Closed symbols indicate ignition (I), open symbols indicate extinction (E)

To compare the catalytic results more clearly, the result curves for different catalysts in the same stage are shown in Fig. 5.12. Although Pd is more active than Pt in the first I-E cycle, methane conversion dropped significantly when water added in in the second I-E cycle. $Pt_{1.6}Pd$

and Pt catalysts have similar performances and $Pt_{1.6}Pd$ is even slightly better than Pt in the whole reaction process. In the hydrothermal aging graph, both of them show good stabilities.

Fig. 5.13 compares conversions and activities of catalysts under FL conditions. TOFs can be formed similarly as under FR conditions:

TOF (Pd, FL) = $4*10^{-4}/0.0114 = 0.035\ s^{-1}$ (versus $0.053\ s^{-1}$ under FR)

TOF (Pt, FL) = $1*10^{-3}/0.0029 = 0.344\ s^{-1}$ (versus $2\ s^{-1}$ under FR)

TOF ($Pt_{1.6}Pd$, FL) = $8.2*10^{-4}/0.0131 = 0.063\ s^{-1}$ (versus $0.176\ s^{-1}$ under FR)

Thus, under FL conditions Pd is only 1 order of magnitude less active than Pt (versus 2 orders under FR conditions). Alloying Pt and Pd improves Pd activity.

Note that both in FL and FR conditions, CH_4 and H_2O concentrations in the feed are the same, only O_2 concentration differs 10 times. The order of O_2 on Pd is reported in the ranges of -0.2 to +0.2 [57], which in our case for Pd is ~ -0.2 to explain the rate increase at lower O_2 concentrations (FR).

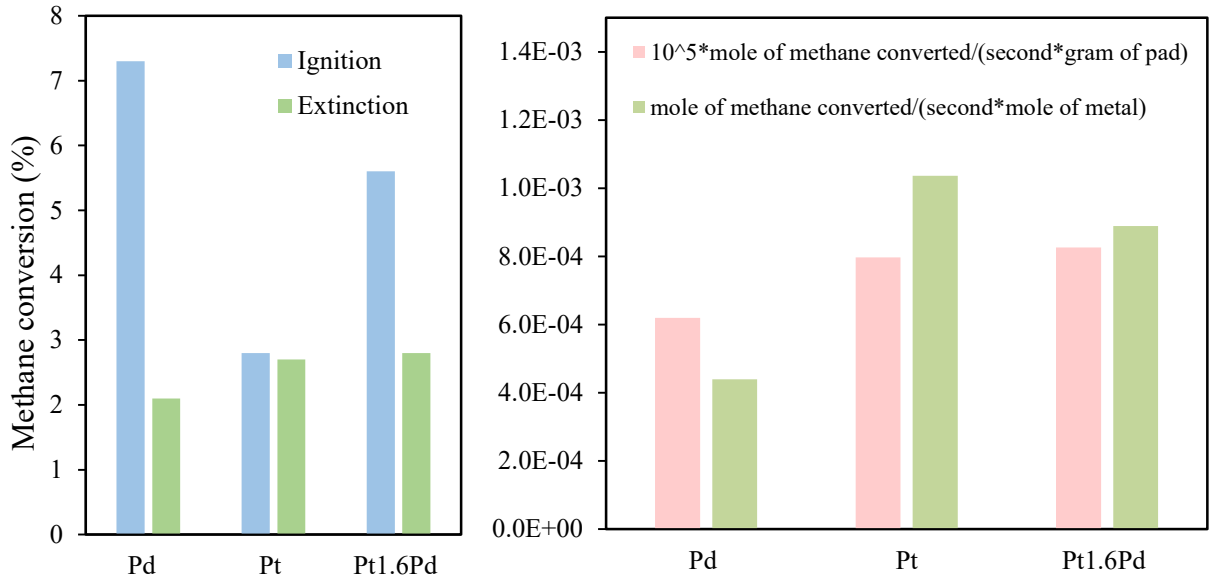

Fig. 5.13. Conversions and activities under fuel-lean conditions.

Fig. 5.14 – 5.16 show comparison of Pt, Pd and $Pt_{1.6}Pd$ catalyst performance under FL vs FR conditions. Under wet conditions, Pd behaves similarly under FL and FR conditions, while Pt performs significantly better under FR conditions than under FL. The bimetallic catalyst also performs better under FR conditions than under FL.

Thus, under the FL conditions, $Pt_{1.6}Pd$ catalyst allowed the same behavior as Pt catalyst (Fig. 5.12). All catalysts show lower conversions at FL conditions vs FR conditions, but Pt out performs Pd in much lower degree under FL conditions. Pt presence is paramount under FR conditions, but becomes of less importance under FL conditions, where it can be successfully replaced by $Pt_{1.6}Pd$.

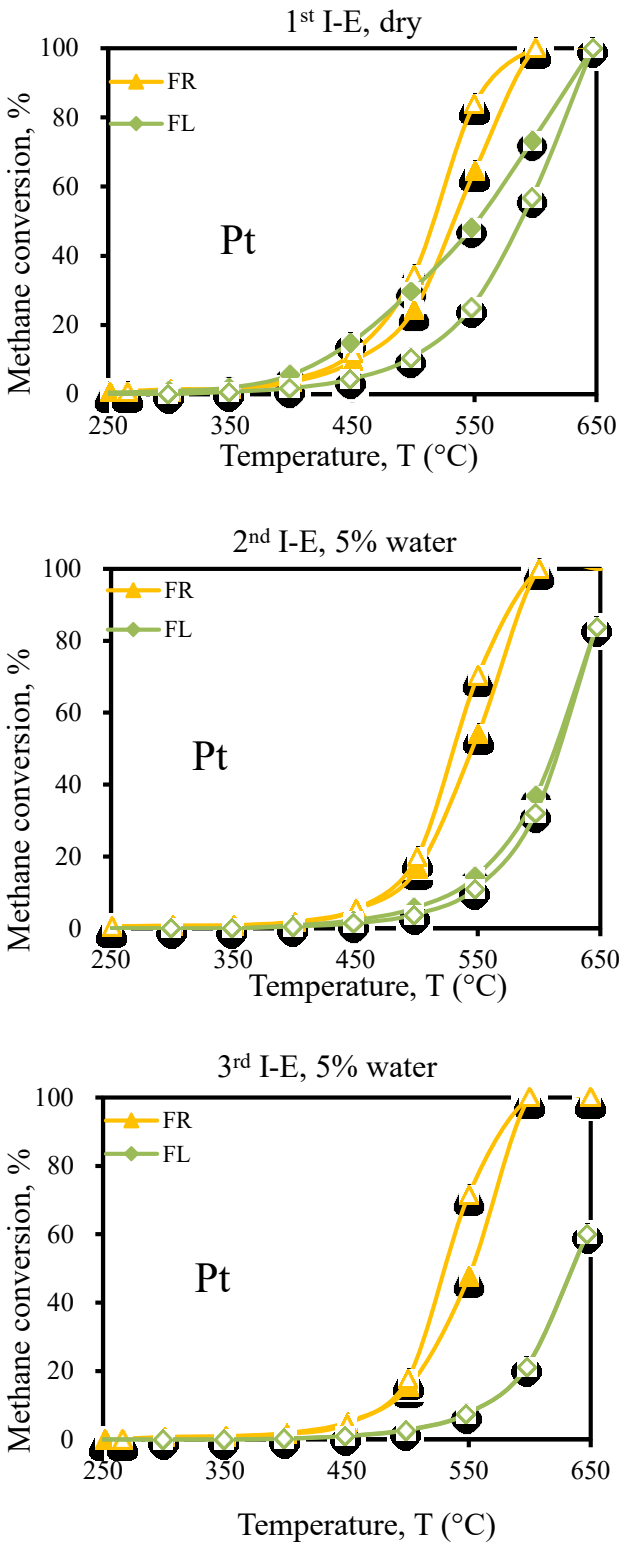

Fig. 5.14. Comparisons of Pt 0.15 wt. % under fuel rich and fuel lean conditions. Closed symbols indicate ignition (I), open symbols indicate extinction (E)

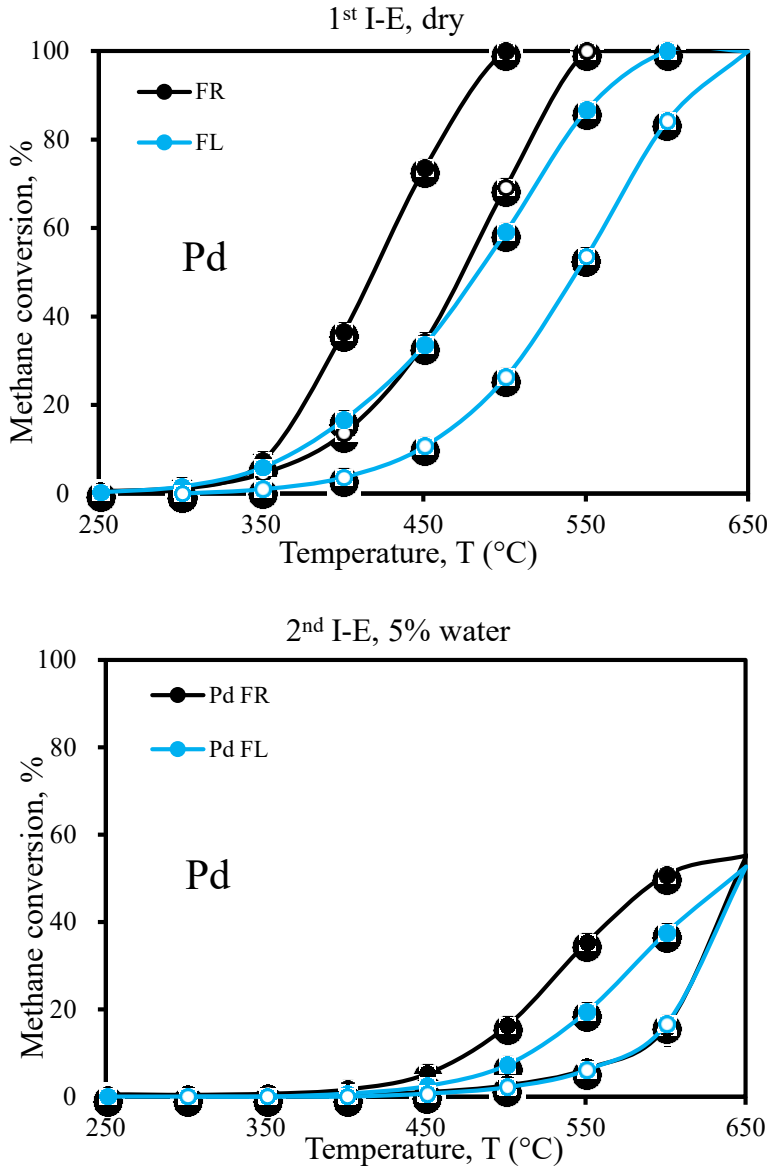

Fig. 5.15. Comparisons of Pd 0.15 wt. % under fuel rich and fuel lean conditions. Closed symbols indicate ignition (I), open symbols indicate extinction (E)

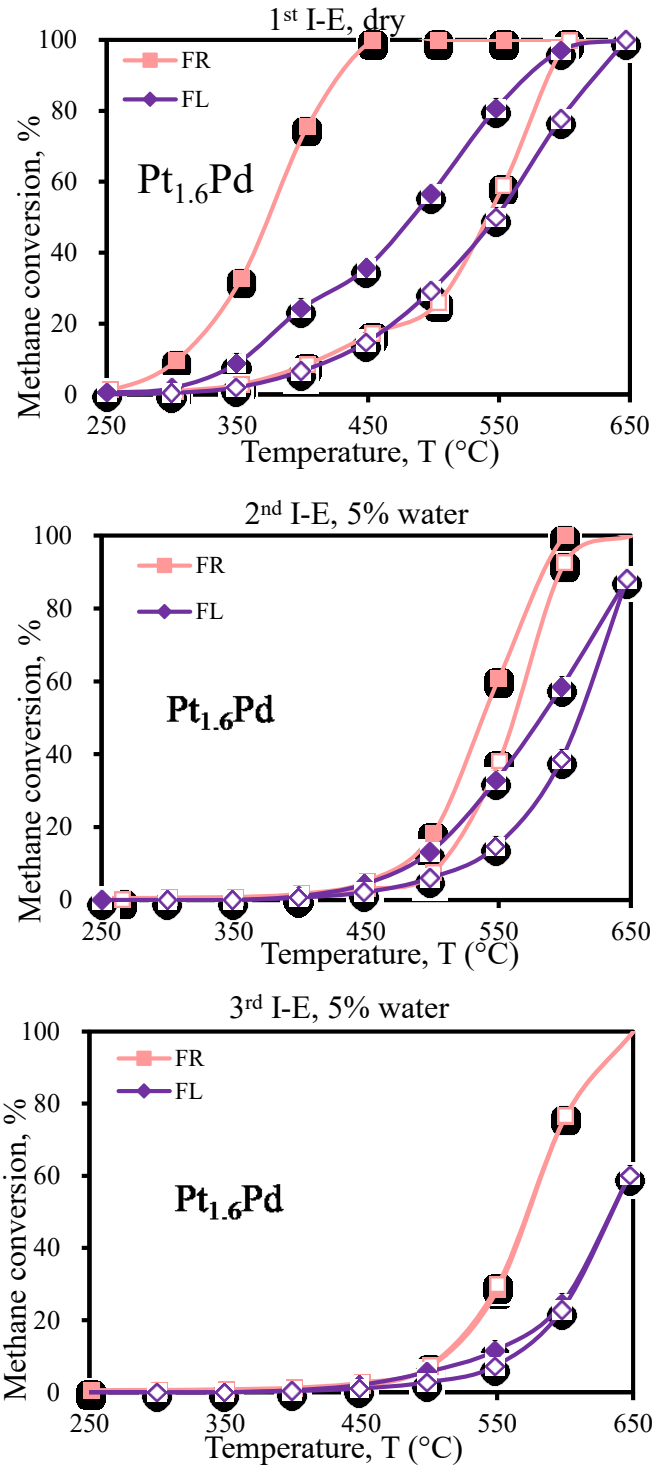

Fig. 5.16. Comparisons of $Pt_{1.6}Pd$ 0.15 wt. % under fuel rich and fuel lean conditions. Closed symbols indicate ignition (I), open symbols indicate extinction (E)

5.5 Recommendations for the industrial heater

Based on the experimental results discussed in Sections 5.1 - 5.4, some recommendations can be given to the catalyst design for a counter-diffusive heater. Figs. 5.17 and 5.18 compare the performance of commercially used monometallic Pt and our suggested $Pt_{1.6}Pd$ catalyst under fuel-rich and fuel-lean conditions, respectively. According to Fig. 5.18, the temperature profile in a counter-diffusive heater is not uniform [7]. Also, the methane to oxygen ratio varies significantly along the reactor based on Fig. 5.18. Thus, in the catalytic pad, there are high and low temperature regions and fuel-rich and fuel-lean regions.

As per Fig. 5.19, approximately 2/3 of the pad thickness is at a temperature above 650 ºC, in the distance of ~0.057 – 0.067 m from the back of reactor. At this distance, according to Fig. 5.19, the pad operates under fuel-rich conditions. At fuel-rich conditions at 650 ºC, the proposed bimetallic pad achieves the same 100% conversion as the commercial active Pt component (Fig. 5.17).

In the lower-temperature part between 0.067 and 0.070 m distance from back of the reactor, the reaction mixture is less saturated with methane and approaches fuel-lean conditions (Fig. 5.20). Under fuel-lean conditions, the proposed bimetallic pad behaves even better than the monometallic Pt pad (Fig. 5.18).

For the temperatures below 650 ºC in the fuel-rich region, the bimetallic pad shows lower conversions (36% versus 52% for Pt at 550 ºC, Fig. 5.17) but shows significantly enhanced stability as opposed to the mono Pt pad. Although not tested for longer time, the trend of Pt catalyst deactivation may be indicative of further conversion drop for the Pt-only pad. Platinum alloying with palladium is beneficial for stability [54], which should be especially advantageous in high-temperature region, when Pt alone forms volatile species and sinters, but Pd addition prevents Pt volatilization.

Thus, the use of $Pt_{1.6}Pd$ catalyst is recommended as a replacement for monometallic Pt. The bimetallic pad provides similar or improved methane conversions, more stable performance,

which may suggest longer life time. This replacement will also result in cost savings for the metal price for one pad as: 16 dollars for the traditional platinum one and only 11 dollars for our new pad.

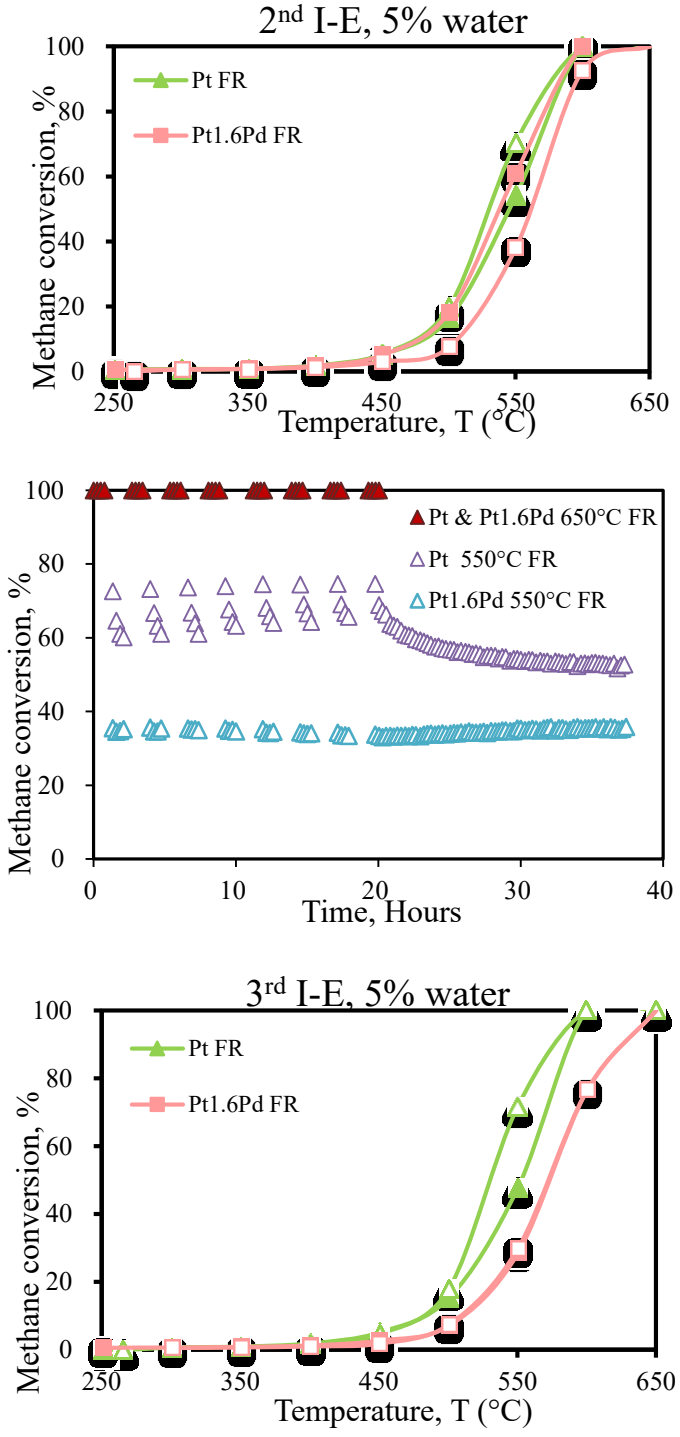

Fig. 5.17. I-E cycles and HTA comparison for Pt and $Pt_{1.6}Pd$ of 0.15 wt. % at FR conditions

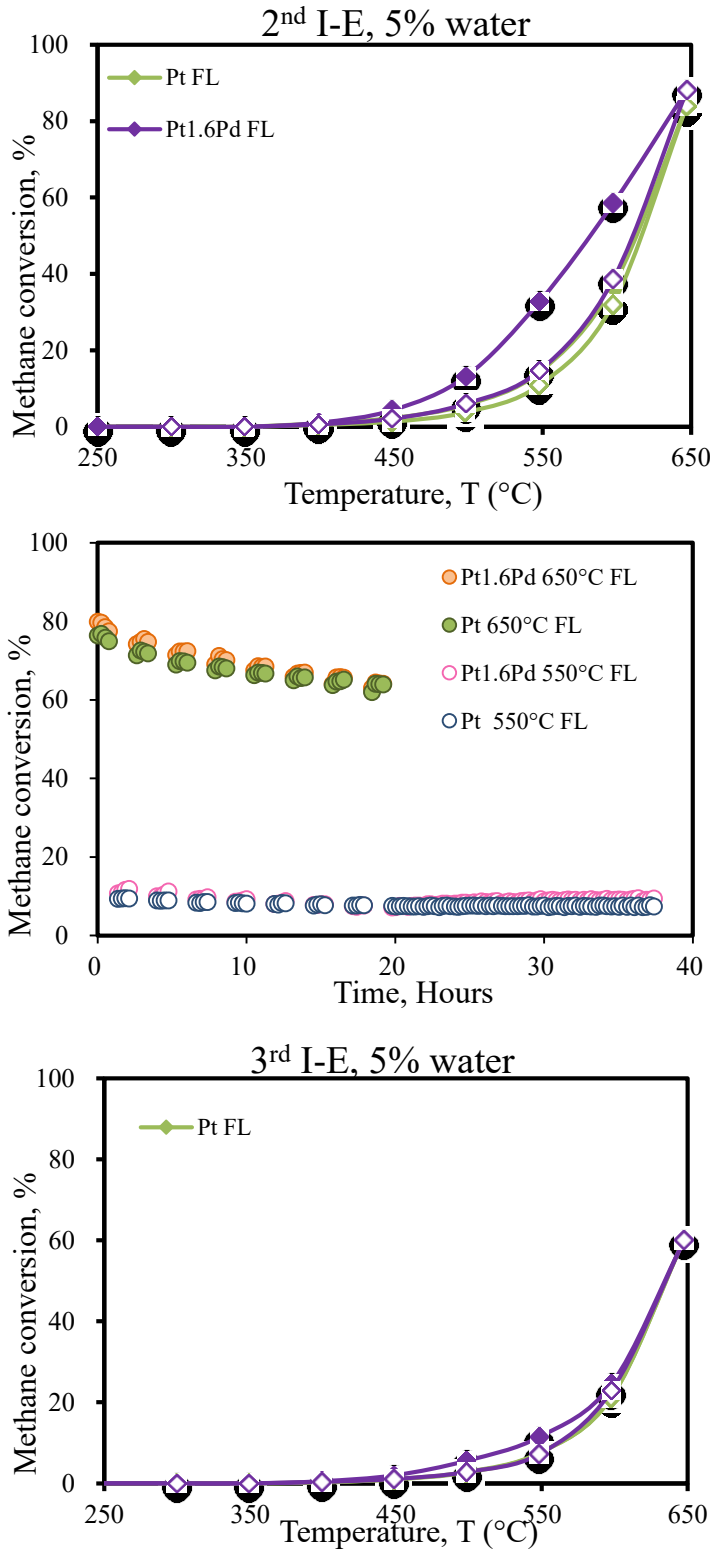

Fig. 5.18. I-E and HTA comparison for Pt and $Pt_{1.6}Pd$ of 0.15 wt. % under FL conditions

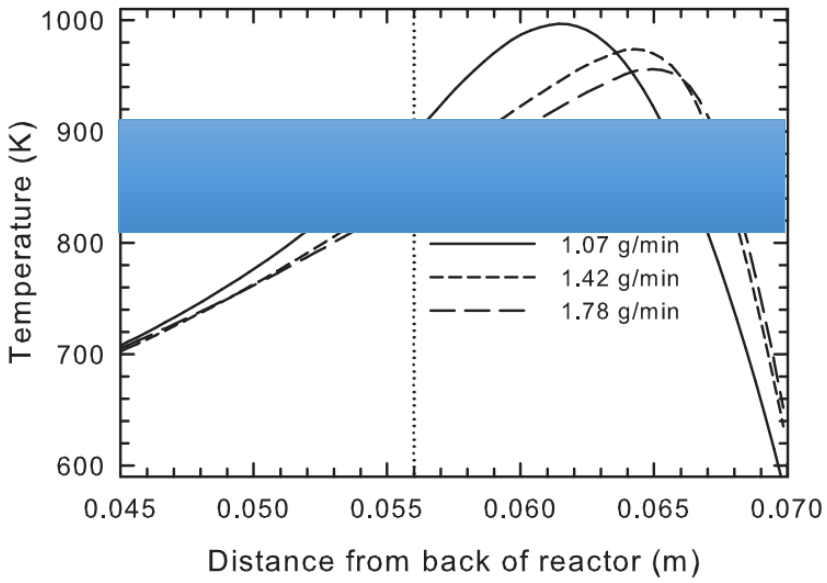

Fig. 5.19. Temperature profiles along the reactor at different methane flow rates. The vertical dotted line marks the position of the interface between insulation blanket and the catalyst pad. The shaded area shows the range of 550 – 650 ºC temperature window, where high methane conversion were obtained as per Fig. 5.17 and 5.18. Reprinted from [7] with permission.

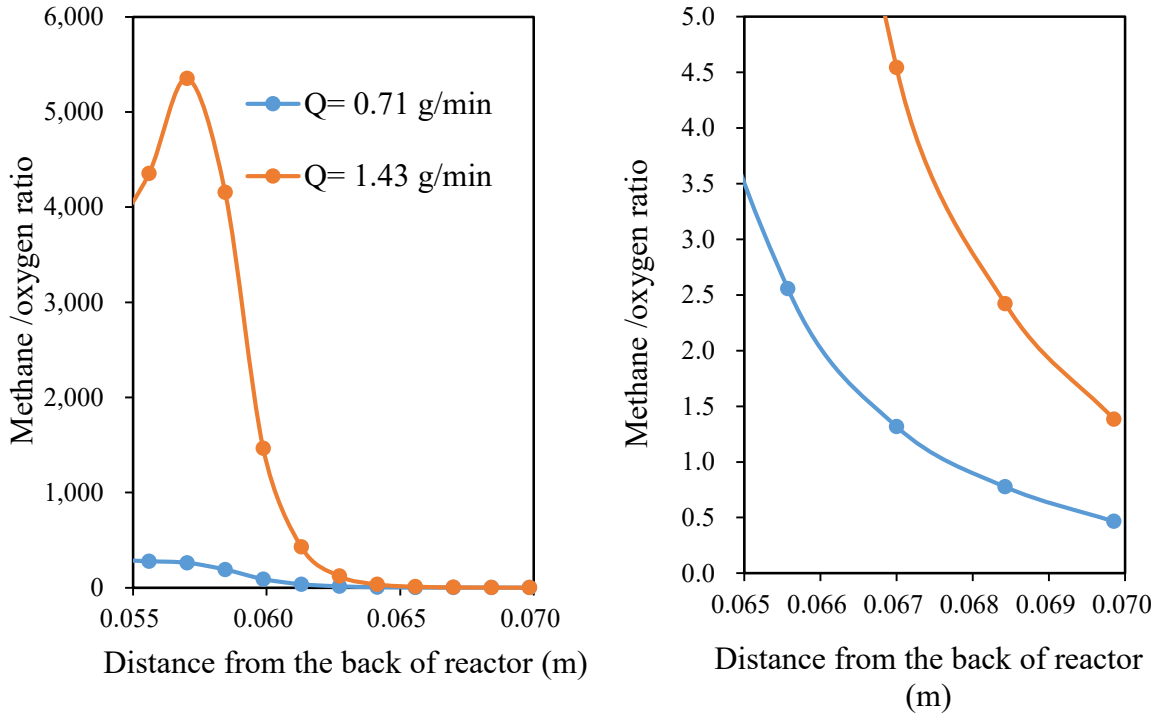

Fig. 5.20. Methane to oxygen molar ratio, calculated based on data from [7]

6. Conclusions

The study aimed to develop alternative catalysts for methane-fuelled catalytic heaters that would be able to replace expensive platinum-containing pads used commercially. Catalytic heaters exhibit significant temperature and reactant/product concentration variations that dramatically affect the catalyst performance. The catalyst must both be stable under high temperature (up 800 °C) and display high activity at low temperatures to ensure complete methane combustion. The current work aimed to replace some of the platinum present in the pads for palladium, which is less expensive. The Pd-Pt catalysts are known for higher thermal stability, but the data on their performance in the presence of water and fuel-rich or fuel-lean conditions are scarce.

In this work, monometallic Pt, Pd and bimetallic Pt-Pd catalysts of different molar ratios were prepared by dry impregnation method and tested under both “fuel-rich” (methane/oxygen molar ratio of 0.2) and “fuel-lean” conditions (methane/oxygen molar ratio of 0.02) to find out the most suitable catalyst. Four stages of experimental procedures were performed during catalyst testing in a flow setup for methane combustion: first ignition and extinction (dry), second ignition and extinction (with 5% water presence), thermal aging from 550 °C to 650 °C (with 5% water present) and third ignition and extinction (with 5% water presence). Both activity and stability were tested.

Under “fuel-rich” conditions, monometallic Pt catalyst has the highest activity. Bimetallic Pt-Pd catalyst with a molar ratio of 1.6:1 is the least expensive catalyst with acceptable activity and also more stable than monometallic Pt catalyst. Under “fuel-lean” condition, bimetallic Pt1.6Pd catalyst has slightly better performance (activity and stability) than monometallic Pt catalyst, while bimetallic Pt1.6Pd is less expensive than monometallic Pt. The catalysts were characterized by TEM and CO chemisorption that revealed improved platinum metal dispersion with palladium addition.

Thus, the use of $Pt_{1.6}Pd$ catalyst is recommended as a replacement for monometallic Pt. The

bimetallic pad provides similar or improved methane conversions, more stable performance, which may suggest longer life time. This replacement mayl also result in cost savings for the metal price for one pad (1 foot * 1 foot * 0.5 inch) as: 16 dollars for the traditional platinum one and only 11 dollars for our new pad.

7. Recommendations for future work

In the current study the catalysts were prepared by dry impregnation of a commercial metal-free pad with dissolved metal precursors. The use of a different support may result in improved activity and/or stability. It is recommended to use higher internal surface area support to improve the metal dispersion.

Because of the time limitations, in the current work only two methane/oxygen ratios were used to test the catalysts. The ratios above stoichiometry (eg, methane to oxygen molar ratio equals 1:3, 1:5, et al) must be assessed as well.

The developed pads may be recommended for testing on a commercial catalytic heater unit to assess their performance.

Reference

[1] D. Ciuparu, M. R. Lyubovsky, E. Altman, L. D. Pfefferle, and A. Datye, "Catalytic Combustion of Methane Over Palladium-Based Catalysts," *Catal. Rev.*, vol. 44, no. 4, pp. 593–649, 2002.

[2] H. Widjaja, K. Sekizawa, K. Eguchi, and H. Arai, "Oxidation of methane over Pd/mixed oxides for catalytic combustion," *Catal. Today*, vol. 47, no. 1–4, pp. 95–101, 1999.

[3] N. Jodeiri, L. Wu, J. Mmbaga, R. E. Hayes, and S. E. Wanke, "Catalytic combustion of VOC in a counter-diffusive reactor," *Catal. Today*, vol. 155, no. 1–2, pp. 147–153, 2010.

[4] "Low Temperature Catalytic Heaters," *Johnson Matthey Technology Review*. .

[5] M. R. Dongworth and A. Melvin, "Diffusive catalytic combustion," *Symp. Int. Combust.*, vol. 16, no. 1, pp. 255–264, 1977.

[6] P. Bröckerhoff and B. Emonts, "Use of natural gas in a catalytic radiant burner for low-emission heat production," *Stud. Surf. Sci. Catal.*, vol. 107, pp. 133–138, 1997.

[7] N. Jodeiri, J. P. Mmbaga, L. Wu, S. E. Wanke, and R. E. Hayes, "Modelling a counter-diffusive reactor for methane combustion," *Comput. Chem. Eng.*, vol. 39, pp. 47–56, 2012.

[8] M. D. Rumminger, R. D. Hamlin, and R. W. Dibble, "Numerical analysis of a catalytic radiant burner: effect of catalyst on radiant efficiency and operability," *Catal. Today*, vol. 47, no. 1–4, pp. 253–262, 1999.

[9] J. H. Lee and D. L. Trimm, "Catalytic combustion of methane," *Fuel Process. Technol.*, vol. 42, no. 2–3, pp. 339–359, 1995.

[10] J. Au-Yeung, K. Chen, A. T. Bell, and E. Iglesia, "Isotopic Studies of Methane Oxidation Pathways on PdO Catalysts," *J. Catal.*, vol. 188, no. 1, pp. 132–139, 1999.

[11] Wyckoff, R.W.G., *Crystal Structures*, 2nd ed., vol. 1, 580. John Wiley and Sons, New York, 1963.

[12] G. Bayer and H. G. Wiedemann, "Formation, dissociation and expansion behavior of

platinum group metal oxides (PdO, RuO_2, IrO_2),” *Thermochim. Acta*, vol. 11, no. 1, pp. 79–88, 1975.

[13] M. Peuckert, “XPS study on surface and bulk palladium oxide, its thermal stability, and a comparison with other noble metal oxides,” *J. Phys. Chem.*, vol. 89, no. 12, pp. 2481–2486, 1985.

[14] J. J. Chen and E. Ruckenstein, “Role of interfacial phenomena in the behavior of alumina-supported palladium crystallites in oxygen,” *J. Phys. Chem.*, vol. 85, no. 11, pp. 1606–1612, 1981.

[15] J. J. Chen and E. Ruckenstein, “Sintering of palladium on alumina model catalyst in a hydrogen atmosphere,” *J. Catal.*, vol. 69, no. 2, pp. 254–273, 1981.

[16] E. Ruckenstein and J. J. Chen, “Spreading and surface tension gradient driven phenomena during heating of alumina-supported palladium crystallites in oxygen,” *J. Catal.*, vol. 70, no. 1, pp. 233–236, 1981.

[17] R. J. Farrauto, J. K. Lampert, M. C. Hobson, and E. M. Waterman, “Thermal decomposition and reformation of PdO catalysts; support effects,” *Appl. Catal. B Environ.*, vol. 6, no. 3, pp. 263–270, 1995.

[18] Y. L. Lam and M. Boudart, “Oxidation of small palladium particles,” *J. Catal.*, vol. 47, no. 3, pp. 393–398, 1977.

[19] S. C. Su, J. N. Carstens, and A. T. Bell, “A Study of the Dynamics of Pd Oxidation and PdO Reduction by H_2 and CH_4,” *J. Catal.*, vol. 176, no. 1, pp. 125–135, 1998.

[20] H. Conrad, G. Ertl, J. Küppers, and E. E. Latta, “Interaction of NO and O_2 with Pd(111) surfaces. I.,” *Surf. Sci.*, vol. 65, no. 1, pp. 235–244, 1977.

[21] S. Jain, T. T. Kodas, and M. Hampden‐Smith, “Oxidation Kinetics of Calcium‐Doped Palladium Powders,” *J. Electrochem. Soc.*, vol. 144, no. 4, pp. 1222–1231, Apr. 1997.

[22] R. Imbihl, “Oscillatory reactions on single crystal surfaces,” *Prog. Surf. Sci.*, vol. 44, no. 3–4, pp. 185–343, 1993.

[23] P. Légaré, L. Hilaire, G. Maire, G. Krill, and A. Amamou, “Interaction of oxygen and

hydrogen with palladium," *Surf. Sci.*, vol. 107, no. 2–3, pp. 533–546, 1981.

[24] C. F. Cullis and B. M. Willatt, "Oxidation of methane over supported precious metal catalysts," *J. Catal.*, vol. 83, no. 2, pp. 267–285, 1983.

[25] F. H. Ribeiro, M. Chow, and R. A. Dallabetta, "Kinetics of the Complete Oxidation of Methane over Supported Palladium Catalysts," *J. Catal.*, vol. 146, no. 2, pp. 537–544, 1994.

[26] Y.-F. Y. Yao, "Oxidation of Alkanes over Noble Metal Catalysts," *Ind. Eng. Chem. Prod. Res. Dev.*, vol. 19, no. 3, pp. 293–298, 1980.

[27] K. Fujimoto, F. H. Ribeiro, M. Avalos-Borja, and E. Iglesia, "Structure and Reactivity of $PdOx/ZrO_2$ Catalysts for Methane Oxidation at Low Temperatures," *J. Catal.*, vol. 179, no. 2, pp. 431–442, 1998.

[28] R. F. Hicks, H. Qi, M. L. Young, and R. G. Lee, "Structure sensitivity of methane oxidation over platinum and palladium," *J. Catal.*, vol. 122, no. 2, pp. 280–294, 1990.

[29] W. G. Rothschild, H. C. Yao, and H. K. Plummer, "Surface interaction in the platinum-.gamma.-alumina system. V. Effects of atmosphere and fractal topology on the sintering of platinum," *Langmuir*, vol. 2, no. 5, pp. 588–593, 1986.

[30] H. Lieske, G. Lietz, H. Spindler, and J. Völter, "Reactions of platinum in oxygen- and hydrogen-treated $Pt\gamma$-Al_2O_3 catalysts: I. Temperature-programmed reduction, adsorption, and redispersion of platinum," *J. Catal.*, vol. 81, no. 1, pp. 8–16, 1983.

[31] R. W. McCabe, C. Wong, and H. S. Woo, "The passivating oxidation of platinum," *J. Catal.*, vol. 114, no. 2, pp. 354–367, 1988.

[32] R. K. Nandi, F. Molinaro, C. Tang, J. B. Cohen, J. B. Butt, and R. L. Burwell Jr., "Pt/SiO_2: VI. The effects of pretreatment on structures," *J. Catal.*, vol. 78, no. 2, pp. 289–305, 1982.

[33] J. L. Gland, B. A. Sexton, and G. B. Fisher, "Oxygen interactions with the Pt(111) surface," *Surf. Sci.*, vol. 95, no. 2–3, pp. 587–602, 1980.

[34] R. F. Hicks, Q.-J. Yen, and A. T. Bell, "Effects of metal-support interactions on the chemisorption of H_2 and CO on $PdSiO_2$ and $PdLa_2O_3$," *J. Catal.*, vol. 89, no. 2, pp. 498–510, 1984.

[35] D. Roth, P. Gélin, A. Kaddouri, E. Garbowski, M. Primet, and E. Tena, “Oxidation behaviour and catalytic properties of Pd/Al_2O_3 catalysts in the total oxidation of methane,” *Catal. Today*, vol. 112, no. 1–4, pp. 134–138, 2006.

[36] R. Burch and P. K. Loader, “Investigation of Pt/Al_2O_3 and Pd/Al_2O_3 catalysts for the combustion of methane at low concentrations,” *Appl. Catal. B Environ.*, vol. 5, no. 1–2, pp. 149–164, 1994.

[37] D. L. Trimm and C.-W. Lam, “The combustion of methane on platinum—alumina fibre catalysts—I: Kinetics and mechanism,” *Chem. Eng. Sci.*, vol. 35, no. 6, pp. 1405–1413, 1980.

[38] D. J. Kaul and E. E. Wolf, “Fourier transform infrared spectroscopy studies of surface reaction dynamics: II. Surface coverage and inhomogeneous temperature patterns of self-sustained oscillations during CO oxidation on $PtSiO_2$,” *J. Catal.*, vol. 91, no. 2, pp. 216–230, 1985.

[39] S. Sharma, D. Boecker, G. J. Maclay, and R. D. Gonzalez, “The simultaneous measurement of support, metal, and gas phase temperatures using an in situ IR spectroscopic technique,” *J. Catal.*, vol. 110, no. 1, pp. 103–116, 1988.

[40] R. Burch, P. K. Loader, and F. J. Urbano, “Some aspects of hydrocarbon activation on platinum group metal combustion catalysts,” *Catal. Today*, vol. 27, no. 1–2, pp. 243–248, 1996.

[41] A. Ersson, H. Kušar, R. Carroni, T. Griffin, and S. Järås, “Catalytic combustion of methane over bimetallic catalysts a comparison between a novel annular reactor and a high-pressure reactor,” *Catal. Today*, vol. 83, no. 1–4, pp. 265–277, 2003.

[42] K. Persson, A. Ersson, A. M. Carrera, J. Jayasuriya, R. Fakhrai, T. Fransson, and S. Järås, “Supported palladium-platinum catalyst for methane combustion at high pressure,” *Catal. Today*, vol. 100, no. 3–4, pp. 479–483, 2005.

[43] K. Persson, A. Ersson, K. Jansson, N. Iverlund, and S. Järås, “Influence of co-metals on bimetallic palladium catalysts for methane combustion,” *J. Catal.*, vol. 231, no. 1, pp. 139–

150, 2005.

[44] T. Ishihara, H. Shigematsu, Y. Abe, and Y. Takita, “Effects of Additives on the Activity of Palladium Catalysts for Methane Combustion.,” *Chem. Lett.*, no. 3, pp. 407–410, 1993.

[45] “Furuya, T., Yamanaka, S., Hayata, T., & Koezuka, J. (1988). U.S. Patent No. 4,731,989. Washington, DC: U.S. Patent and Trademark Office.”

[46] C. Kul Ryu, M. Wong Ryoo, I. Soo Ryu, and S. Kyu Kang, “Catalytic combustion of methane over supported bimetallic Pd catalysts: Effects of Ru or Rh addition,” *Catal. Today*, vol. 47, no. 1–4, pp. 141–147, 1999.

[47] S. H. Oh and P. J. Mitchell, “Effects of rhodium addition on methane oxidation behavior of alumina-supported noble metal catalysts,” *Appl. Catal. B Environ.*, vol. 5, no. 1–2, pp. 165–179, 1994.

[48] P. Reyes, A. Figueroa, G. Pecchi, and J. L. G. Fierro, “Catalytic combustion of methane on Pd–Cu/SiO_2 catalysts,” *Catal. Today*, vol. 62, no. 2–3, pp. 209–217, 2000.

[49] P. Gélin and M. Primet, “Complete oxidation of methane at low temperature over noble metal based catalysts: a review,” *Appl. Catal. B Environ.*, vol. 39, no. 1, pp. 1–37, 2002.

[50] Y. Deng and T. G. Nevell, “Non-steady activity during methane combustion over Pd/Al_2O_3 and the influences of Pt and CeO_2 additives,” *Catal. Today*, vol. 47, no. 1–4, pp. 279–286, 1999.

[51] H. Yamamoto and H. Uchida, “Oxidation of methane over Pt and Pd supported on alumina in lean-burn natural-gas engine exhaust,” *Catal. Today*, vol. 45, no. 1–4, pp. 147–151, 1998.

[52] K. Narui, H. Yata, K. Furuta, A. Nishida, Y. Kohtoku, and T. Matsuzaki, “Effects of addition of Pt to PdO/Al_2O_3 catalyst on catalytic activity for methane combustion and TEM observations of supported particles,” *Appl. Catal. Gen.*, vol. 179, no. 1–2, pp. 165–173, 1999.

[53] C. Micheaud, P. Marécot, M. Guérin, and J. Barbier, “Preparation of alumina supported palladium–platinum catalysts by surface redox reactions. Activity for complete hydrocarbon oxidation,” *Appl. Catal. Gen.*, vol. 171, no. 2, pp. 229–239, 1998.

[54] T. R. Johns, R. S. Goeke, V. Ashbacher, P. C. Thüne, J. W. Niemantsverdriet, B. Kiefer, C. H. Kim, M. P. Balogh, and A. K. Datye, "Relating adatom emission to improved durability of Pt–Pd diesel oxidation catalysts," *J. Catal.*, vol. 328, pp. 151–164, 2015.

[55] R. Abbasi, G. Huang, G. M. Istratescu, L. Wu, and R. E. Hayes, "Methane oxidation over Pt, Pt:Pd, and Pd based catalysts: Effects of pre-treatment," *Can. J. Chem. Eng.*, vol. 93, no. 8, pp. 1474–1482, 2015.

[56] "Fiberfrax Durablanket S EN.pdf." [Online]. Available: http://www.unifrax.com/web/Audit.nsf/ByUNID/FB7E1D63FB97097285257E900070DF4B/$File/Fiberfrax%20Durablanket%20S%20EN.pdf. [Accessed: 28-Jul-2015].

[57] R. Gholami, M. Alyani, and K. J. Smith, "Deactivation of Pd Catalysts by Water during Low Temperature Methane Oxidation Relevant to Natural Gas Vehicle Converters," *Catalysts*, vol. 5, no. 2, pp. 561–594, Mar. 2015.